ИНСТИТУТ ЯДЕРНОЙ ФИЗИКИ СО АН СССР

V.V. Mirnov, A.J. Lichtenberg

MULTIPLE MIRROR PLASMA CONFINEMENT

PREPRINT 91-116

НОВОСИБИРСК

CONTENTS

INTRODUCTION

Together with toroidal systems, which now hold a leading position in controlled thermonuclear fusion research, an important place also belongs to open plasma confinement systems. Because of their geometrical simplicity and technological advantages they are considered as one of the main alternative concepts for a thermonuclear reactor.

During the last twenty years considerable progress has been made in developing new types of open systems, which possess improved longitudinal confinement in comparison with the "classical" single cell mirror [1, 2]. The plasma lifetime in a single cell mirror is roughly equal to the ion-ion collision time, which is marginal for a fusion reactor. Furthermore, if microfluctuations are exited in the plasma, due to the non-Maxwellian velocity distribution, then scattering on these fluctuations can transport velocities into the mirror loss cone, with corresponding deterioration the reactor power characteristics. Since the level of fluctuation needed for significant enhancement only exceeds the level of thermal fluctuations by a few times, simple open systems, are very sensitive to the presence of high frequency microinstabilities. Our present understanding is not sufficient to insure that known methods of stabilization of these microinstabilities will be effective under thermonuclear reactor parameters. Therefore one of the central aspects of open system investigation is to search for methods of confinement for which the longitudinal losses are not strongly effected by the influence of microinstabilities.

One concept for improving this situation is that of the Tandem Mirror [3, 4]. In this concept a long central cell has improved ion confinement due to electrostatic

forces arising from the higher density end cells. This improves the basic confinement, while at the same time flux from the central cell may inhibit microinstabilities by partially plugging the loss cone. The conditions for inhibiting the instabilities are delicate, and experimental results were not as favorable as theoretical predictions.

Another solution to this problem is to have an open system whose length exceeds the mean free path of the charged particles. Under this condition the velocity space distribution function is close to an equilibrium Maxwellian which therefore eliminates the thermodynamic drive for a wide class of microinstabilities. This makes the physics of plasma confinement simpler and therefore allows more reliable predictions of the various confinement schemes. However, to have a device of reasonable length the value of the mean free path must be radically reduced, requiring both low temperature and high density. The practical realization of a device in this temperature and density range also requires the reduction of energy and particle flux to the ends of the machine. One possibility of achieving this reduction consists in corrugating the magnetic field, so that the flux becomes diffusive rather than a free interial flow. Configurations of this type have been called "corrugated open traps" or "multiple mirrors."

A multiple mirror consists of a set of mirrors which are connected to each other at their ends and have a full length L which exceeds the mean free path λ of the particles. If, at the same time, the corrugation period $l < \lambda$ then a transiting ion will be trapped in one of the mirrors, due to Coulomb collisions, before it leaves the plasma. When after a few oscillations it again becomes transiting, the direction of its longitudinal velocity changes with respect to its initial velocity in a random way. The resulting

motion of ions is therefore a random walk with characteristic space step λ and time interval λ/v_{Ti}. As a result the free inertional plasma flow in a uniform magnetic field turns into slow diffusional expansion along the corrugated magnetic field, which is described by the law

$$z^2 \sim Dt \sim (\lambda v_{Ti})t$$

The effect of the reduction of the plasma expansion rate can be interpreted in another way as the result of the friction of transiting particles colliding with the trapped particles. The latter ones give their momentum to the magnetic field. One should emphasize that in a straight magnetic field the diffusive process is not possible because the collision of a pair of ions does not change their total momentum; in a corrugated field such scattering results in trapping in mirrors with high probability (i.e. the loss of the total momentum) with corresponding decrease of the plasma expansion velocity. This effect allows a considerable reduction in the length and energy input in a reactor based on multiple mirror confinement. The multiple mirror concept has the additional very useful property that if the confinement time (and therefore the reactor Q) falls short of predictions, the desired values can be recovered by making the device a little longer, with τ_{conf} improving proportionally to L^2.

We now give a brief history of the idea of multiple mirror confinement. The term "corrugated field" has been mentioned in papers on plasma physics over a long period, (see, for example [5]) but this work is not directly related to axial confinement. A mechanism similar to that of multiple mirror confinement was discussed in [6], which analyzes the slowing down of longitudinal plasma motion inside of a dense pinch plasma, by use of rough walls. A boundary between plasma and magnetic field

with $\beta = 1$, i.e. no field inside the plasma, was considered, and particle motion in the transverse direction was limited by reflection from the corrugated magnetic surface. Another statement of the problem was considered in [7], where the effect on confinement of a single mirror by adding additional cells was studied. The approach taken in [7] was based on the Monte-Carlo calculations of particle behavior in the corrugated field with fixed scattering centers. In connection with this model we should note that a fixed scattering center model can produce diffusion even in a straight magnetic field, so the diffusive character of plasma expansion in a corrugated field cannot be confirmed using a fixed centers model. As to the results of [7], because the plasma temperature and density were chosen such that $\lambda \gg L$ the wrong conclusion was made that there is a linear dependence of lifetime on the number of mirrors. This was pointed out in [8], where the fixed centers model was used in the proper mean free path regime, so that the correct quadratic dependence of lifetime on number of mirrors was found. The result was consistent with that obtained in a different problem in which r.f. induced scattering in small mirror cells was investigated [9]. Although this result was based on the fixed centers model and is therefore not rigorous it was intuitively clear that trapped particles would behave similar to fixed scattering; thus, it encouraged the authors to pursue a self-consistent treatment of multiple mirror confinement [10].

Independently from this work, being carried out in Berkeley, at approximately the same time a self-consistent analysis of multiple mirror confinement was performed by a group in Novosibirsk [11] that contained a quantitatively precise description of the effect of the corrugation. The diffusion equation for plasma density that was first given

in [11] was derived from the full set of kinetic equations based on actual *ii*, *ee*, and *ei* collisions. The detailed presentation of the theory appeared in [12]. The mathematical methods needed for the construction of this theory, was partly based on the papers published earlier under the study of the problems of electroconductivity of inhomogeneous plasma [13] and skin-effect in corrugated magnetic field [14, 15]. However, the consideration of some aspects of multiple mirror theory, particulary the construction of macroscopic equations for plasma parameters, required the creation of new methods.

In summary, the concept of multiple mirror confinement was independently invented and developed in Novosibirsk and Berkeley from the beginning of 70's. From that time until the present it has been extensively studied from both theoretical and experimental points of view as a new method of longitudinal plasma confinement. The bibliography of multiple mirror systems now numbers more than 100 papers. Since the basic studies in this field are reasonably complete it appears to be an appropriate time to present a detailed description of the results. The main attention in the present review is on the results of axial loss theory.

Since the plasma parameters during the expansion along the field vary considerably, the theory should cover this wide parameter range. In Section 1 the various regimes of reduction of the plasma expansion rate are qualitatively discussed, the velocities of plasma motion are estimated, and the regimes are classified depending on the mean free path, the length of corrugation and mirror ratio.

A rigorous theory of longitudinal plasma flow in a corrugated magnetic field is given in Sections 2 and 3. In Section 2 the method of construction of flow equations

is described for the case when the particle motion within the length of each mirror can be considered as collisionless (e.g. with small-scale corrugations). Although, in this regime, the flow of plasma does not obey the ordinary two-fluid gas dynamic equations, the smallness of λ compared with the scale of longitudinal inhomogeneity (which can normally be assumed equal to L) is sufficient for the flow of the plasma to be described macroscopically by means of moment equations.

The investigation of the opposite limiting case of collisional cells (regime of large-scale corrugation) is presented in Section 3. For the case of large-scale corrugations, when the mean free path is small in comparison with the period of the corrugation, the two fluid gas dynamic equations can be used to describe the motion. Besides the pure gas dynamic case the theory of an "intermediate" regime, which is realized in a magnetic field with narrow collisionless mirrors ("point" mirrors) is discussed as well. Since there are a number of different regimes, it is useful to construct a single approximate equation which covers them. Such an equation proved to be effective, for example, in the analysis of the problem of reducing the length and energy of the reactor due to inserting a small amount of heavy impurities with $Z >> 1$.

In order to be useful as a controlled fusion device, the multiple mirror confinement scheme must have a reactor embodiment that is feasible, i.e., one that operates with reasonable magnetic field strengths, lengths, and average powers. Although the results of the basic confinement studies at Novosibirsk and Berkeley gave similar results [10, 12], two quite different reactor embodiments were conceived. The Novosibirsk group considered a pulsed reactor concept with dense plasma (10^{17}—10^{18} cm^{-3}) heated by means of relativistic electron beams. Since at the high density and thermonuclear temperature, megagaus fields are required for magnetic

confinement, the alternate radial confinement mechanism of "wall" confinement (β >> 1) is considered, for which the magnetic field suppresses only the transverse thermal conductivity, but equilibrium in this direction is provided by the rigid walls. The length is kept short due to the high density ($n \sim 10^{17} cm^{-3}$) and the average power and wall loading is maintained at a reasonable level by having a low duty cycle. The concept was put forth and developed in a series of papers, which we reference in Section 4.1.

In contrast, the Berkeley group considered a steady-state reactor with β <1. The highest feasible superconducting magnetic fields were used in the central cell to have high density ($n \sim 10^{16} cm^{-3}$), to keep the length short, and employing a few relatively large mirrors. The average power was high but could be partly controlled with the plasma radius. The concept was set out and further developed in a series of papers referenced in Section 4.3.

Because of the very different reactor concepts, ancillary physics, required to validate the concept, also took different paths. For the pulsed concept, major concerns were the effectiveness of the magnetic insulation, and the maintenance of the on-axis mirror ratio, both arising from the high β operation. These concerns were addressed in a series of papers, which we reference in Section 4.2. For the steady-state concept the major ancillary concern was MHD stability. Since a multiple mirror is, at best, avarage minimum B, the conditions for stability and the design of appropriate magnetic field structures, particulary for the large mirror ratios, becomes quite difficult. Early work considered low β stability, while later work also dealt with ballooning modes. We reference these studies in Section 4.4.

The early theoretical results of the longitudinal confinement encouraged parallel experimental efforts in Novosibirsk and Berkeley to confirm the results. These experiments employed alkali plasmas that were easy to produce and could operate in a density-temperature regime in which multiple mirror confinement could clearly be observed in small laboratory experiments. MHD stability was insured by line-tying to a cathode at which the plasmas was generated. The results of these experiments confirmed the main aspects of multiple mirror confinement theory, although in a regime very different from the usual fusion experiments.

Following the early quite similar results, the experimental work in the Berkeley and Novosibirsk groups diverged, in accordance with the reactor concepts being considered. The Berkeley group was interested in investigating combined confinement and MHD stability in a more realistic, but still scaled, density and temperature regime ($n_e \approx 10^{13} \text{cm}^{-3}$, $T_e = T_i \approx 10$ eV). Plasma was injected into the center of the device, either from one or both ends, and allowed to decay. Linked quadrupole fields, built according to the results of the low β stability calculations, were employed. Two devices of lengths 3 meters with 7 cells and, later, 10 meters with 10 cells were employed. The results, particularly in the large machine, were consistent with the multiple mirror confinement calculations and indicated stability up to $\beta \approx 1$, as predicted. The Novosibirsk group was interested in creating plasmas with $\beta > 1$ on axis, requiring novel plasma injection and heating schemes. This work has led to the development of a 7 meter electron beam-plasma interaction experiment with plans to increase the length and install multiple mirrors. These experimental investigations are referenced in Section 5, where the results are presented. This is followed by a summary and conclusions.

1. QUALITATIVE CONSIDERATION OF MULTIPLE MIRROR EFFECTS

The main developments of the physics of multiple mirror confinement were obtained in the process of investigation of the possibility of creating a thermonuclear reactor with a dense plasma (dense in the sense that the mean free path λ is small compared with the length L of the system). To estimate what effect the corrugation of the magnetic field can have on such a reactor we first consider a simpler system consisting of a magnetic field without corrugation. Although both pulsed and steady-state variants can be considered, for simplicity we concentrate our attention on a pulsed system. Following [16] let us take a long solenoid with a straight magnetic field in which a relatively short bunch of hot ($T \simeq 10$ keV) dense plasma is prepared at $t = 0$. This bunch then freely expands along a magnetic field for $t > 0$. If the magnetic field suppresses the transverse transport then the time of energy containment is determined by the time of longitudinal expansion $\tau \equiv L/v_{Ti}$, where v_{Ti} is the thermal ion velocity (which holds when there is no contact between plasma and the ends of the device). During plasma expansion a thermonuclear reaction in a bunch takes place and this system is effective as a reactor, if $n\tau > 10^{14}$ sec-cm^{-3}, where n is a characteristic density. In terms of limitation on the length L it means

$$nL > 3.10^{22} \text{ cm}^{-2} \tag{1.1}$$

It shows that even if the characteristic density is very high, $n \simeq 10^{17}$ cm^{-3} (the initial bunch has considerably higher n), the length of reactor, based at free plasma expansion, should be not less than 3000 m. A reactor with these parameters, both because of the high plasma pressure and high power needed for heating, is not

technically feasible.

As already mentioned in the introduction, a dramatic improvement in longitudinal confinement can be obtained with a corrugated magnetic field (see Fig. 1). Considering that the longitudinal and transverse problems of plasma confinement can be considered separately, the longitudinal confinement problem is reduced to specifying initial density and temperature distribution along a magnetic field line and then describing the space and time plasma parameter evolution. We use this approach to qualitatively consider the different regimes of plasma flow in a corrugated magnetic field and estimate the velocity of expansion and confinement time as a function of mean free path λ, corrugation length l and mirror ratio k. To explore the complete parameter range, requires investigation of the various limiting cases:

$$\lambda/l \begin{cases} \gg 1, \\ \ll 1, \end{cases} \quad k-1 \begin{cases} \gg 1 \\ \ll 1. \end{cases}$$

These four possibilities are not all of equal significance, as we shall see below and in the following sections. The intermediate values are approached by extrapolation of the limiting cases. We classify these regime first by λ/l, designating $\lambda/l \gg 1$ as the regime of "small scale corrugation" and $\lambda/l \ll 1$ as the regime of "large scale corrugation." Secondarily we designate $k \gg 1$ as the regime of "strong corrugation" and $k - 1 \ll 1$ as the regime of "weak corrugation." In exploring these limiting cases we shall also find some sub-cases of interest for which explicit calculations can be made. In addition, particularly for the lower density steady-state concepts, it is desirable to construct cells with "point" mirrors, i.e. with a mirror scale length $l_m \ll l$, such that it is possible to operate in the regime $l_m \ll \lambda - l$, which has improved confinement properties.

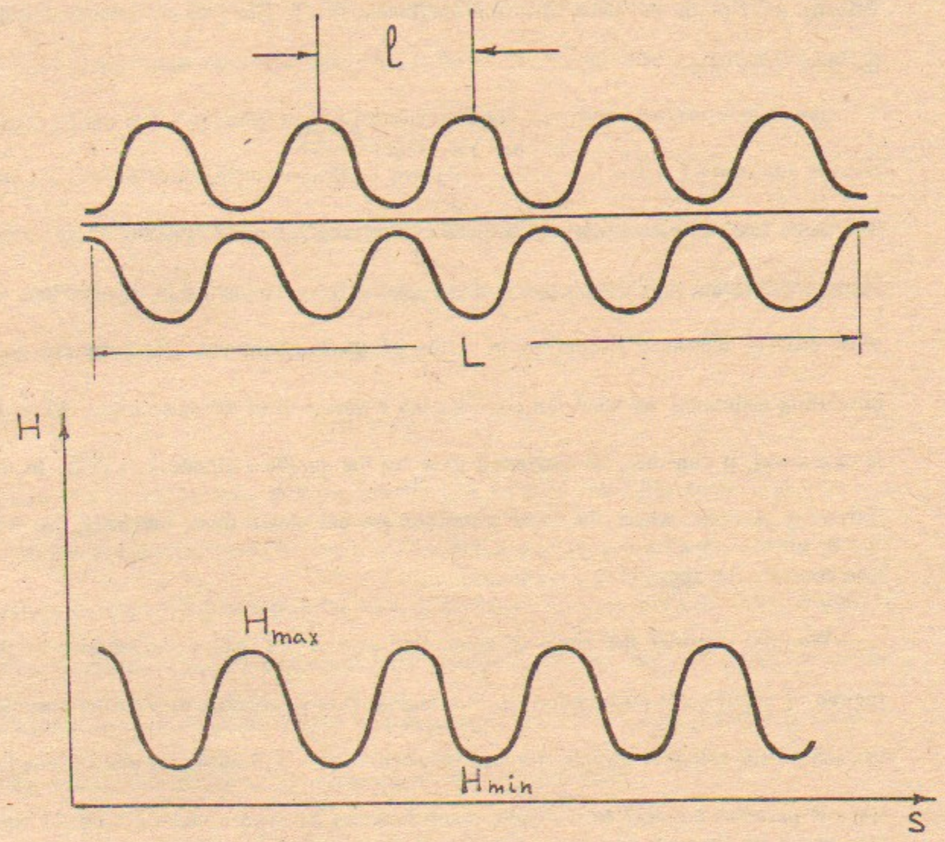

Figure 1. Multiple-mirror magnetic trap
(a) the geometry of the force lines
(b) the strength of the magnetic field on the axes of the system.

We also note that because λ varies inversely with n, various regimes of λ/l can exist within a given device.

The axial confinement in the device can be characterized either by the local flow velocity $u(z)$ or by the local diffusion coefficient $D(z)$. The two are related through the flow, such that

$$n(z)u(z) = -D(z)\frac{dn(z)}{dz}$$

Sometime one representation, and sometimes the other, is more convenient for calculating confinement. For the purposes of the qualitative examination in this section, we shall express the local properties in terms of u. Furthermore, since we are only presenting estimates, we shall not consider the z-variation of the quantities. When D is calculated, it can then be converted to u by the simple estimate $u = D/L$. In the following sections, where the local quantities are calculated more precisely, we will also consider the appropriate z-variations.

We first consider the range of mean free path $\lambda \gg l$ which we classify as the regime of small scale corrugation. In this regime it is reasonable to separate particles in each mirror cell into particles trapped between mirrors and transiting ones. Since the trapped particles are able to complete many bounces between mirrors during the time between two successive collisions they make only a small contribution to the mass and energy transport, i.e. the plasma flow along the axis is mostly carried by the transiting particles. Consequently the friction occurs between the transiting particles and the trapped particles and the latter transmit the momentum received to the magnetic field. Therefore one can say that the plasma undergoes friction with the magnetic field.

In the case of not-too-large mirror ratio, $k - 1 \sim 1$, the frictional force on a particle can be estimated as

$$F_{f_r} \simeq m_i \nu_{ii} u'$$

where m_i is the mass of an ion, ν_{ii} is the ion-ion collision frequency (in case $k - 1 \sim 1$ this determines the time needed for transiting particles to scatter through an angle of the order of unity and to become trapped, i.e. lose its momentum), and u' is the directed velocity of the transiting particles, which at $k - 1 \sim 1$ coincides in order of magnitude with the macroscopic flow velocity of the plasma. Equating $n F_{f_r}$, which is the friction force acting on unity plasma volume, with plasma pressure gradient $\partial p/\partial z \sim nT/L$, we find the expansion rate

$$u' \sim \nu_{Ti}(\lambda/L) \ll \nu_{Ti}$$

From this it can be seen that the introduction of even relatively small k $(k - 1 \sim 1)$ corrugation causes a marked reduction of u, and a corresponding increase in the plasma expansion time compared with the case of a smooth field. In fact the very character of motion changes: inertial expansion with a velocity $u \sim \nu_{Ti}$ becomes diffusion of the plasma from one magnetic mirror cell to another and the pressure gradient is counterbalanced by the friction of the plasma with the magnetic field.

A larger mirror ratio further limits the expansion rate by reducing (i) the number of transiting particles and (ii) their effective free path length. The first effect results from the fact that since the trapped particles, the number of which is k times greater than of the transit ones, on average are not in motion, the mass velocity of the plasma as a whole is smaller than u' by a factor k. The second effect results from the fact

that, when $k \gg 1$, for capture in a cell to occur it is sufficient for a transiting particle to be scattered through a small angle $\Delta\theta^2 \sim k^{-1}$. Therefore the effective mean free path and effective collision frequency, that determine the time of the momentum loss of the transiting particles, become of the order of λ/k and $\nu_{ii}k$, respectively. For this reason "smallness" of a magnetic mirror trap length must be taken to mean:

$$l \ll \lambda/k \tag{1.2}$$

As a result of these two effects the expansion velocity decreases with high mirror ratio by a factor k^2.

$$u \sim v_{Ti}(\lambda/k^2 L) \tag{1.3}$$

A reduction of the expansion velocity occurs even with very weak corrugation $k - 1 \ll 1$. In this case those particles are trapped for which a pitch-angle θ at the minimal magnetic field is close enough to $\pi/2$,

$$|\theta - \frac{\pi}{2}| \leq (k-1)^{1/2}, \tag{1.4}$$

so the time of transition from trapped particles into transiting ones is of the order of magnitude $(k-1)/\nu_{ii}$. In a classification of different regimes with weak corrugation, the regime of small cell length, when the transition time exceeds the bounce time of trapped particles in single mirror trap $l/v_{Ti}(k-1)^{1/2}$ we call the small-scale corrugation regime. This regime exists when

$$l \ll \lambda(k-1)^{3/2}, \tag{1.5}$$

where we have taken into account that in mirror trap with weak corrugation the longitudinal velocity of trapped particles is of the order of $v_{Ti}(k-1)^{1/2}$.

The effect of a weak corrugation can be found by introducing the frictional force related to one particle that can be estimated from reasoning quite similar to that described above for the situation with $k \gg 1$. The only difference is that now the characteristic time for the transiting particle to lose it's momentum increases correspondingly to the decrease in probability for it to find itself in the narrow interval of pitch angles (1.4). This time increases as $\nu_{ii}^{-1}(k-1)^{-1/2}$. Taking this into account one can easily derive the following expression for F_{fr}:

$$F_{fr} = -m_i \nu_{ii}(k-1)^{1/2} u.$$

Equating $n F_{fr}$ with the plasma pressure gradient, we estimate the expansion rate as

$$u \sim v_{Ti}\lambda/L(k-1)^{1/2} \ll v_{Ti}. \tag{1.6}$$

From (1.6) one can see that if both (1.5) and the limitation $\lambda \ll L(k-1)^{1/2}$ are satisfied then the expansion rate is much smaller than the thermal velocity.

We now consider the intermediate mean free path regime for weak corrugation. If the mean free path becomes smaller than given by the inequality (1.5), the expansion rate ceases to depend on the collision frequency. In this range of parameters the time of exchange between trapped and transiting particles becomes smaller than a period of trapped particle oscillations. The mechanism of transfer of momentum from plasma to magnetic field is quite analogous the a usual collisionless Landau damping. An effect of this kind is also found in "neoclassical" theory of transport in toroidal devices creating the "plateau" regime [17]. As is known from the solution of the Landau damping problem, the frictional force between particles and wave is proportional to square of the amplitude of modulation. The condition of the balance of frictional force

and pressure gradient allows one to estimate the expansion velocity as

$$u \sim v_{Ti}\, l/L(k-1)^2, \tag{1.7}$$

which shows that in the range $l \ll L(k-1)^2$ the weak corrugation substantially decreases the plasma flow velocity in comparison with the straight magnetic field case.

If one continues to decrease the mean free path, there is a transition to a third mean free path regime which is strongly collisional and for which the expansion rate can be found from two-fluid gas dynamic equations. In this regime the flow is impeded as a result of the longitudinal ion viscosity. This interval of parameters which corresponds to very small (in the sense noted above) mean free path we define as the regime of large-scale corrugation, or alternatively as the viscous fluid regime.

To estimate the plasma expansion rate in this regime let us consider the plasma flow in an individual magnetic mirror cell. The motion of the plasma is due to the pressure difference between the ends of the cell, which is equal in order of magnitude to nTl/L. The work of the pressure force is balanced by viscous dissipation and, with strong enough magnetic field, only longitudinal viscosity is significant. The energy dissipated per unit time within the trap is

$$\eta_i S \int_0^l \left[\frac{\partial u}{\partial z}\right]^2 dz \sim \eta_i S\, u^2(k-1)^2/l, \tag{1.8}$$

where η_i is the coefficient of longitudinal ion-ion viscosity [18], which is given approximately by $\eta_i \sim n\, m_i\, v_{Ti}\, \lambda$, and S is the characteristic transverse plasma cross-section. In the estimation of the integral in (1.8) we take into consideration that the variation of u along the length of single mirror cell is approximately determined by

the variation ΔS of the cross-section S: $\Delta u/u \sim \Delta S/S \sim k-1$. Comparing (1.8) with the work performed per unit time by the pressure forces, $SunTl/L$, we find the plasma velocity to be

$$u \sim v_{Ti}\, l^2/\lambda L(k-1)^2 \tag{1.9}$$

Comparing (1.7) and (1.9) one can conclude that the regime of large-scale corrugation is realized if $\lambda \ll l$. Certainly all results presented above are valid only if $u \ll v_{Ti}$; in the opposite case the inertial effects are of major importance.

Equating the flow in the plateau regime, given by (1.7) to the flow in the small and large scale corrugation regimes, given by (1.6) and (1.9), respectively, we find that the plateau exists for

$$\frac{l}{(k-1)^{3/2}} \le \lambda \le l$$

When the mirror ratio increases this interval gets shorter and if $k-1 \sim 1$ it disappears. The optimal confinement is realized in this situation with $\lambda \sim l$ which separates the cases of small-scale and large-scale corrugations. A summary of the different regimes considered above is presented in Fig. 2, that qualitatively explore the dependence of the plasma expansion velocity on the factor λ/l for both the cases of weak $k-1 \ll 1$ and moderate $k-1 \sim 1$ values of mirror ratio. It should be noted that for $k-1 \sim 1$ the expansion velocity is considerably decreased in comparison with the thermal velocity even if $\lambda < l$ (up to $\lambda \sim l^2/L$).

The classification given above is related to the geometry of a magnetic force line with a single scale, that is, when the areas with weak and strong magnetic field have

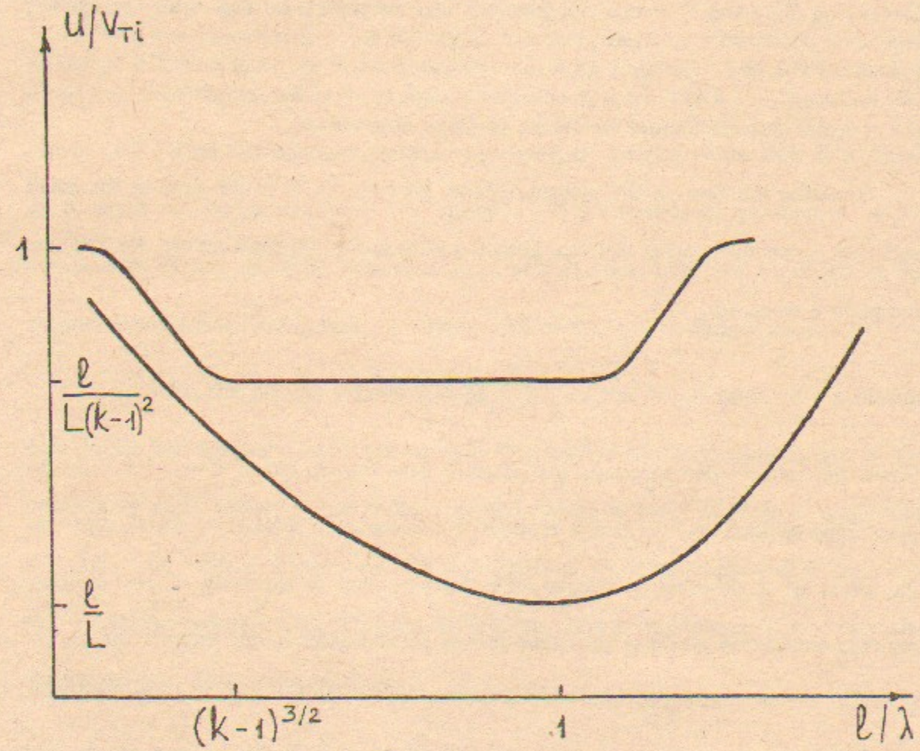

Figure 2. Qualitative dependence of the plasma expansion velocity on the factor l/λ
(a) the case of weak corrugation $k - 1 \ll 1$;
(b) the case of moderate corrugation $k - 1 \sim 1$.

approximately the same length. A better geometry from a practical point of view has narrow mirrors, i.e. a scale length l_m of the strong magnetic field which is much smaller than l. In this case of a two-scale field geometry there is an intermediate range of mean free paths $l_m \ll \lambda \ll kl$, when the plasma flow inside the individual mirror cells is pure gas dynamical but particles move without collision through the mirrors.

Let us consider an individual mirror cell with $l_m \ll l$. The rate of plasma losses through a mirror throat can be estimated as $n\, v_{Ti}\, S_{\min}$, where $S_{\min}$ is the plasma cross-section in the throat. Dividing the total amount of ions in the mirror cell nlS by the loss rate, one obtains an estimate of the particle lifetime in the individual mirror cell as kl/v_{Ti}. After this time the ion leaves one of the mirror traps in a random direction becomes trapped in an adjacent cell such that the space step of this random motion is equal to l and time interval is equal to kl/v_{Ti}; the diffusion coefficient can then be estimated as $D \sim v_{Ti} l/k$. An estimate of plasma expansion velocity in this "intermediate" regime is then

$$u \sim D/L \sim v_{Ti}(l/kL). \tag{1.10}$$

Comparing (1.10) to (1.3) we see that the two expressions are equal for $\lambda/k = l$. This is a considerable reduction of the velocity from the "single scale" mirror satisfying (1.2). This regime has been called the "ideal" multiple mirror regime.

Let us now analyze qualitatively the improvement of a pulsed reactor, discussed at the beginning of this section due to a multiple mirror geometry. If one takes, for example, the expression (1.3) or (1.10) for the expansion velocity, estimating the plasma life-time $\tau \sim L/u$, and substituting it in Lawson criteria for a temperature of 10 keV, the following limitation for the length of the system is obtained:

$$nL > 2.10^{21}/k \text{ cm}^{-2} \qquad (1.11)$$

Comparing (1.1) with (1.11) we see that with the same densities the corrugation allows a reduction of the length of approximately a factor of 10 k. Finding such a strong effect warrants a more accurate theory, the development of which will be given in the following sections.

2. PLASMA FLOW IN A MAGNETIC FIELD WITH SMALL-SCALE CORRUGATION

In the regime of small scale corrugation, $\lambda \gg l$, the diffusive process is directly related to the scattering of ions in velocity space, which transfers them between trapped and passing distributions. A kinetic description is required to adequately describe this regime. Various approximations have been used to make these kinetic equations tractable, in fact, in the limit of $k \gg 1$, a simple geometric approximation, in which the magnetic field effects depend only on K, gives reasonably accurate values for the local diffusion coefficient [11]. The most systematic kinetic treatment was presented in [13], and extended to weak corrugations in [21]. We follow these presentations here. The derivation of the equations for the averaged plasma parameters is presented in Section 2.1. It is based on the expansion of the kinetic equation solutions in the small parameter λ/L. The mass and energy fluxes are determined from the first order corrections to Maxwellian distributions. They can be calculated analytically in the case of a high mirror ratio in the presence of ii, ee, and ei collisions. The possibility of simplifying the collisional terms results first from the smallness of the number of transiting particles and second from the narrow interval of pitch-angles occupied by transiting particles in velocity space.

The equations for the first order corrections, simplified in this way, are solved in Section 2.2 by expansion in another small parameter l/λ with average over a single mirror cell similar to the method suggested in [22]. The solution of these equations allows one to find the mass and energy fluxes and to get a closed system of diffusive

equations for macroscopic plasma parameters. The analysis of the properties of this equations is carried out in Section 2.3.

For a weakly modulated magnetic field the regime of small-scale corrugation corresponds to the case (1.5), when the trapped particles' period of oscillation is much longer than the transit time of untrapped ones. The analysis of this case has similar features to the well-known problem of finite amplitude Langmuir wave collisional damping [23]. The effect of the interaction of the particles with weakly corrugated magnetic field is given by an expression for the frictional force, which is derived in Section 2.4

2.1 Derivation of the Macroscopic Equation

In the limit of small-scale corrugation (1.2) the plasma motion does not obey the two-fluid gas dynamic equations [18]. However, as was shown in [12] the smallness compared with the scale of axial inhomogeneity L is sufficient to enable the flow of the plasma to be described macroscopically by means of moment equations.

We shall regard the magnetic field as large enough to enable us to neglect (i) all transport phenomena perpendicular to the lines of force and (ii) any change in the magnetic field caused by the plasma itself. Given these conditions, the state of the plasma inside an individual field tube is described by the following pair of kinetic equations:

$$\frac{\partial F_a}{\partial t} + v\,\cos\theta\,\frac{\partial F_a}{\partial s} + \frac{v\,\sin\theta}{2H}\,\frac{\partial H}{\partial s}\,\frac{\partial F_a}{\partial \theta}$$

$$\pm\frac{e}{m_a}E_{\parallel}\left[\cos\theta\,\frac{\partial F_a}{\partial v} - \frac{\sin\theta}{v}\,\frac{\partial F_a}{\partial \theta}\right] = \sum_b St_{ab} \qquad (2.1)$$

Here v is the particle velocity, θ is the angle between the velocity vector and the direction of the magnetic field, s is a co-ordinate along the line of force, $F_a \equiv F_a(v,\theta,s,t)$ is a distribution function (the subscript $a = i, e$ denotes the type of particle), $E_{\parallel}$ is a projection of the electric field onto a line of force, St_{ab} is the collision operator between species a and b and the other notation is standard. The plus sign before the last term on the left-hand side of the equation refers to ions and the minus sign to electrons. It is assumed that the corrugation length is large compared with the Larmor electron and ion radii.

The required system of gas dynamic equations is obtained from expression (2.1) by an expansion in the parameter λ/L, where L represents the characteristic scale of inhomogeneity of the plasma. Here we shall regard $E_{\parallel}$ as a first order quantity with respect to λ/L (since the electric field is created by an electron pressure gradient). In the zero approximation with respect to λ/L (i.e. in a plasma that is uniform along the line of force and has no electric field) equations (2.1) have a steady-state solution in the form of two Maxwellian distributions:

$$F_{Ma} = n_a\left[\frac{m_a}{2\pi T_a}\right]^{3/2}\exp\left[-\frac{m_a v^2}{2T_a}\right]. \qquad (2.2)$$

Contrary to normal two-fluid gas dynamics, the macroscopic velocity is a small quantity (first order with respect to λ/L (see expression (1.3)) which means that the solution of the zero approximation for each type of particle is characterized by only two parameters, n_a and T_a. It should be noted in particular that we consider $T_e \neq T_i$,

since the temperature equalization time contains the large parameter m_i/m_e.

If the Maxwellian distribution parameters n_a and T_a vary along the line of force, functions (2.2) cease to be accurate solutions of the kinetic equations. Accurate solutions are then best written in the form

$$F_a = F_{Ma} + f_a \tag{2.3}$$

where the parameters of the Maxwellian function F_{Ma} are determined from the relations

$$n_a = 2\pi \int_0^\infty v^2 dv \int_0^\pi \sin\theta\, F_a\, d\theta,$$
$$T_a = \frac{2\pi m_a}{3n_a} \int_0^\infty v^4 dv \int_0^\pi \sin\theta\, F_a\, d\theta$$

and f_a is a small additional term associated with the inhomogeneity and proportional to λ/L. It will be obvious, then, that

$$\int_0^\infty v^2 dv \int_0^\pi \sin\theta\, f_a\, d\theta = 0, \quad \int_0^\infty v^4 dv \int_0^\pi \sin\theta\, f_a\, d\theta = 0$$

For practical applications the most interesting case is that of strong corrugation ($k \gg 1$), and fortunately it is precisely here that we can obtain relatively easily a closed system of gas dynamic equations. Therefore, from now on we shall consider that $k \gg 1$.

Let us examine a section of the field tube located between two mirrors (Fig. 1). Since the plasma parameters vary little over the length of one magnetic mirror trap, the state of the plasma within this section can be adequately described by the mean densities and temperatures over the section:

$$\bar{n}_a = \frac{H_{\max}}{ll} \int_{s_1}^{s_2} \frac{n_a(s)ds}{H(s)}, \quad \bar{T} = \frac{H_{\max}}{ll\bar{n}_a} \int_{s_1}^{s_2} \frac{n_a(s)T_a(s)ds}{H(s)} \tag{2.4}$$

where

$$l = \frac{H_{\max}}{l} \int_{s_1}^{s_2} \frac{ds}{H(s)}$$

and integration with respect to ds is performed from mirror to mirror. Using the kinetic equations (2.1) together with the definitions (2.4) it can easily be shown that

$$\frac{\partial \bar{n}_a}{\partial t} + \frac{q_a(s_2) - q_a(s_1)}{ll} = 0 \tag{2.5}$$

$$\frac{\partial n_a \bar{T}_a}{\partial t} + \frac{2}{3} \frac{Q_a(s_2) - Q_a(s_1)}{ll} \mp \frac{2e\, H_{\max}}{3ll} \int_{s_1}^{s_2} \frac{E_{\parallel}(s)\, q_a(s)\, ds}{H(s)} = 0 \tag{2.6}$$

where the quantities

$$q_a = 2\pi \int_0^\infty v^3 dv \int_0^\pi f_a \sin\theta \cos\theta\, d\theta,$$
$$Q_a = \pi m_a \int_0^\infty v^5 dv \int_0^\pi f_a \sin\theta \cos\theta\, d\theta$$

are, respectively, the mass and energy fluxes. In Eq. (2.6) we have omitted terms of two types: (i) terms which describe the temperature exchange between electrons and ions and (ii) terms which appear in the event of directional motion of any of the components and describe the energy dissipation due to mutual friction forces between electrons and ions. We have neglected terms of the second type as they are small when $k \gg 1$. As regards temperature equalization, this can be allowed for directly in the final moment equations.

In view of the small variation of all the plasma parameters along the magnetic mirror trap, it is convenient to introduce the quantities

$$\frac{\partial q_a}{\partial z} = \frac{q_a(s_2) - q_a(s_1)}{l}, \quad \frac{\partial Q_a}{\partial z} = \frac{Q_a(s_2) - Q_a(s_1)}{l} \tag{2.7}$$

with which we can operate formally as with ordinary derivatives. Here instead of expression (2.5) and (2.6) we have:

$$\frac{\partial \bar{n}_a}{\partial t} + \frac{1}{l}\frac{\partial q_a}{\partial z} = 0 \tag{2.8}$$

$$\frac{\partial \bar{n}_a \bar{T}_a}{\partial t} + \frac{2}{3}\frac{1}{l}\frac{\partial Q_a}{\partial z} \mp \frac{2e H_{\max}}{3Il}\int_{s_1}^{s_2} \frac{E_{\parallel}(s) q_a(s)\, ds}{H(s)} = 0 \tag{2.9}$$

Let us now find the functions f_a. The derivative $\partial F_a/\partial t$ is a quantity of the second order of smallness. Therefore the equation for determining f_a, obtained by substituting expression (2.3) in (2.1), takes the following form (accurate to terms of first order):

$$\begin{aligned} \hat{D} f_a &\equiv v\cos\theta \frac{\partial f_a}{\partial s} + \frac{v\sin\theta}{2H}\frac{\partial H}{\partial s}\frac{\partial f_a}{\partial \theta} \\ &= \sum_b St'_{ab} - v\cos\theta\frac{\partial F_{Ma}}{\partial s} \mp \frac{eE_{\parallel}}{m_a}\cos\theta\frac{\partial F_{Ma}}{\partial v} \end{aligned} \tag{2.10}$$

where St'_{ab} denotes the result of linearization of St_{ab} with respect to f_a.

The variation of f_a over the length of a magnetic mirror cell is a quantity of second order, so that the boundary condition for Eq. (2.10) can be written as

$$f_a(s_2) - f_a(s_1) = 0 \tag{2.11}$$

Since $E_{\parallel}$ is a quantity of the first order, in the last term on the right-hand side of equation (11) we can neglect the variation of F_{Ma} over the magnetic mirror trap and put

$$\frac{\partial F_{Ma}}{\partial v} = -\frac{m_a v}{T_a}\bar{F}_{Ma}$$

where $\bar{F}_{Ma}$ represents a Maxwellian distribution with averaged parameters

$$\bar{F}_{Ma} = \bar{n}_a\left(\frac{m_a}{2\pi T_a}\right)^{3/2}\exp\left(-\frac{m_a v^2}{2T_a}\right)$$

Similarly, it can be assumed that

$$\frac{\partial F_{Ma}}{\partial s} = \left[\frac{1}{\bar{n}_a}\frac{\partial n_a}{\partial s} + \frac{1}{T_a}\frac{\partial T_a}{\partial s}\left(\frac{m_a v^2}{2\bar{T}_a} - \frac{3}{2}\right)\right]\bar{F}_{Ma}$$

As already pointed out, when the condition $l \ll \lambda/k$ applies, mass and energy can be transported only by transiting particles. Therefore, to find q_a and Q_a we need to know f_a only in that region of the phase space corresponding to transit particles. Using the small parameter k^{-1}, it is possible to obtain from expression (2.10) a simplified system of equations for transit particles. The principal simplification is associated with the fact that, when $k \gg 1$, there are few transit particles and the collisions between them can be neglected. Moreover, the collision integrals need retain only those terms in which there are two differentiations with respect to θ (the other terms do not contain the large parameter $\Delta\theta^{-2} \sim k$). As shown in papers [13, 15] it is then possible to write St'_{ee} and St'_{ii} for transit particles as follows:

$$St'_{ee} = \frac{\nu\alpha_e(v)}{\sin\theta}\frac{\partial}{\partial\theta}\sin\theta\frac{\partial f_e}{\partial\theta}$$

$$St'_{ii} = \left(\frac{m_e}{m_i}\right)^2\frac{\nu\alpha_i(v)}{\sin\theta}\frac{\partial}{\partial\theta}\sin\theta\frac{\partial f_i}{\partial\theta}$$

where

$$\alpha_a(v) = \frac{4\pi}{\bar{n}}\left[\int_0^v \left(v'^2 - \frac{v'^4}{3v^2}\right)F_{Ma}(v')\,dv' + \frac{2}{3}\int_v^\infty v\,v'\,F_{Ma}(v')dv'\right]$$

$$\nu = \frac{2\pi\Lambda e^4\bar{n}}{m_e^2 v^3}$$

(Λ is the Coulomb logarithm). We have explicitly allowed for quasi-neutrality of the plasma and put $n_e = n_i = \bar{n}$.

The second simplification lies in the fact that for transit ions one can neglect St'_{ie} in comparison with St'_{ii}, since when there is not too large a difference between T_e and T_i, the transit ions exchange momenta and energy with trapped ions much more effectively than with electrons. The final simplification is that for the purpose of calculating St'_{ei} the ions may be regarded as immobile:

$$St'_{ei} = \frac{\nu}{\sin\theta}\frac{\partial}{\partial\theta}\sin\theta\frac{\partial f_e}{\partial\theta}$$

Taking all the above into account, one can write the following equations for determining f_e and f_i in the region of transit particles:

$$\hat{D}f_e = \frac{\nu(1+\alpha_e)}{\sin\theta}\frac{\partial}{\partial\theta}\sin\theta\frac{\partial f_e}{\partial\theta} - \nu\cos\theta\,\bar{F}_{Me}\frac{\partial\phi_e}{\partial s} \qquad (2.12)$$

$$\hat{D}f_i = \left[\frac{m_e}{m_i}\right]^2\frac{\nu\alpha_i}{\sin\theta}\frac{\partial}{\partial\theta}\sin\theta\frac{\partial f_i}{\partial\theta} - \nu\cos\theta\,\bar{F}_{Mi}\frac{\partial\phi_i}{\partial s} \qquad (2.13)$$

$$\phi_a = \frac{n_a}{\bar{n}_a} + \frac{T_a}{\bar{T}_a}\left[\frac{m_a v^2}{2\bar{T}_a} - \frac{3}{2}\right] \mp \frac{e}{T_a}\int_{s_1}^{s_2} E_{\parallel}\,ds$$

2.2 Calculation of the Distribution Function Correction

First we shall solve Eq. (2.12). To do this, we represent f_e as the sum of the two functions p_e and r_e, respectively even and odd with respect to $\cos\theta$

$$f_e = p_e + r_e$$

$$p_e = \frac{1}{2}[f_e(\theta) + f_e(\pi-\theta)],\quad r_e = \frac{1}{2}[f_e(\theta) - f_e(\pi-\theta)]$$

and proceed from expression (2.12) to the following pair of equations for p_e and r_e:

$$\hat{D}p_e = \frac{\nu(1+\alpha_e)}{\sin\theta}\frac{\partial}{\partial\theta}\sin\theta\frac{\partial r_e}{\partial\theta} - \nu\cos\theta\,\bar{F}_{Me}\frac{\partial\phi_e}{\partial s} \qquad (2.14)$$

$$\hat{D}r_e = \frac{\nu(1+\alpha_e)}{\sin\theta}\frac{\partial}{\partial\theta}\sin\theta\frac{\partial p_e}{\partial\theta}. \qquad (2.15)$$

To find f_e it is sufficient to solve Eqs. (2.14) and (2.15) over the interval $[0, \pi/2]$.

Since the scale of variation of the magnetic field is small compared with the free-path length, it is appropriate in equations (2.14) and (2.15) to introduce the variables $\varepsilon = m_e v^2/2$ and $\mu = m_e v^2\sin^2\theta/2H$, which are integrals of the motion of charged particles in a magnetic field. The advantage of such a substitution in this kind of problem was pointed out some years ago [22]. Thus in place of expression (2.14) and (2.15) we obtain

$$\frac{\partial p_e}{\partial s} = \frac{\sqrt{8m_e}\,\nu(1+\alpha_e)}{H}\frac{\partial}{\partial\mu}\left[\mu(\varepsilon-\mu H)^{1/2}\frac{\partial r_e}{\partial\mu}\right] - \bar{F}_{Me}\frac{\partial\phi_e}{\partial s} \qquad (2.16)$$

$$\frac{\partial r_e}{\partial s} = \frac{\sqrt{8m_e}\,\nu(1+\alpha_e)}{H}\frac{\partial}{\partial\mu}\left[\mu(\varepsilon-\mu H)^{1/2}\frac{\partial p_e}{\partial\mu}\right]. \qquad (2.17)$$

Equations such as these have been solved in other studies [13, 15, 24] in connection with other problems (calculation of the conductivity of inhomogeneous plasma and plasma in a corrugated magnetic field). The solution is based on the use of the small parameter l/λ. An expansion of the function p_e and r_e in powers of l/λ takes the form

$$p_e = A + B(l/\lambda)^2 + \ldots, \quad r_e = \frac{C}{(l/\lambda)} + D(l/\lambda) + \ldots$$

As can be seen from expression (2.17) $\partial r_e/\partial s \sim l/\lambda$. This means that the function r_e may be considered constant over the magnetic mirror trap with a relative accuracy of $\sim(l/\lambda)^2$. Allowing for this, we integrate Eq. (2.16) with respect to ds from mirror to mirror. As a result of this, and taking expression (2.11) into account, we obtain

$$\sqrt{8m_e}\,\nu(1+\alpha_e)\frac{\partial}{\partial\mu}\left\{\mu\left[\int_{s_2}^{s_1}\frac{(\varepsilon-\mu H)^{1/2}\,ds}{H}\right]\frac{\partial r_e}{\partial\mu}\right\} = \overline{F}_{Me}[\phi_e(s_2)-\phi_e(s_1)]$$

The solution of this equation, which is finite when $\mu \to 0$, is elementary:

$$r_e = \frac{\overline{F}_{Me}[\phi(s_2)-\phi(s_1)]}{\sqrt{8m_e}\,(1+\alpha_e)\nu} \times \int_{\varepsilon/H_{\max}}^{\mu} d\mu'\left[\int_{s_1}^{s_2}\frac{(\varepsilon-\mu' H)^{1/2}\,ds}{H}\right]^{-1} + C(\varepsilon)$$

The function $C(\varepsilon)$ is determined from the condition that r_e should vanish at the transit-trapped particle boundary (i.e. when $\varepsilon = \mu H_{\max}$). This boundary condition is given more formal treatment elsewhere [13, 23]. It can easily be seen that it gives $C(\varepsilon) = 0$.

With a large mirror ratio ($k \gg 1$) the integral with respect to ds in the formula for r_e is expressed in terms of the quantity I, introduced previously, and is equal to $I\,\varepsilon^{1/2} l/H_{\max}$. In view of this we can write

$$r_e = \frac{\overline{F}_{Me}[\phi(s_2)-\phi(s_1)]}{\sqrt{8m_e}\,(1+\alpha_e)\nu\varepsilon^{1/2} I l}\,(\mu H_{\max}-\varepsilon)$$

Knowing r_e, we can determine the electron mass and energy fluxes after integrating with respect to ε and μ.

The scheme for finding the ion fluxes does not present any new difficulties. The final results of all the calculations can be written in the following form:

$$q_a = -\frac{H}{H_{\max}}\frac{\chi_a I}{\overline{T}_a}\sum_{n=1}^{3}\beta_a^{(n)}\overline{P}_a^{(n)} \tag{2.18}$$

$$Q_a = -\frac{H}{H_{\max}}\chi_a I\sum_{n=1}^{3}\gamma_a^{(n)}\overline{P}_a^{(n)} \tag{2.19}$$

where the coefficient χ_a is determined by the formula

$$\chi_a = \frac{\overline{T}_a^{7/2}}{m_a^{1/2}\Lambda e^4 I^2} \tag{2.20}$$

The remaining symbols in expressions (2.18) and (2.19) are defined in the Table I, where e_m and i_m are expressed as integrals:

$$e_m = \frac{1}{\sqrt{2\pi^3}}\int_0^\infty\left[x^2+\frac{xe^{-x^2}}{\sqrt{\pi}}+\frac{1}{\sqrt{\pi}}(2x^2-1)\int_0^x e^{-\xi^2}\,d\xi\right]^{-1} e^{-x^2}x^m\,dx$$

$$i_m = \frac{1}{\sqrt{2\pi^4}}\int_0^\infty\left[xe^{-x^2}+(2x^2-1)\int_0^x e^{-\xi^2}\,d\xi\right]^{-1} e^{-x^2}x^m\,dx$$

The numerical values of these integrals are

TABLE 1. INTEGRAL VALUES

n	$\beta_e^{(n)}$	$\beta_i^{(n)}$	$\gamma_e^{(n)}$	$\gamma_i^{(n)}$	$\bar{P}_a^{(n)}$
1	$-e_9$	i_9	$-e_{11}$	i_{11}	$\dfrac{e\bar{E}}{\bar{T}_a}$
2	e_9	i_9	e_{11}	i_{11}	$\dfrac{1}{\bar{n}_a}\dfrac{\partial \bar{n}_a}{\partial z}$
3	$e_{11}-\dfrac{3}{2}e_9$	$i_{11}-\dfrac{3}{2}i_9$	$e_{13}-\dfrac{3}{2}e_{11}$	$i_{13}-\dfrac{3}{2}i_{11}$	$\dfrac{1}{\bar{T}_a}\dfrac{\partial \bar{T}_a}{\partial z}$

$e_9 = 0.207$ $\quad e_{11} = 0.81$ $\quad e_{13} = 4.01$

$i_9 = 0.455$ $\quad i_{11} = 1.74$ $\quad i_{13} = 8.47$

The quantities $\bar{E}$, $\partial \bar{n}_a/\partial z$, $\partial \bar{T}_a/\partial z$ in the last column of the table are defined by analogy with the formulae in expression (2.7):

$$\bar{E} = \frac{1}{l}\int_{s_1}^{s_2} E_{\parallel}\, ds, \qquad \frac{\partial n_a}{\partial z} = \frac{n(s_2) - n(s_1)}{l}$$

$$\frac{\partial T_a}{\partial z} = \frac{T_a(s_2) - T_a(s_1)}{l}$$

Substituting relations (2.18) and (2.19) in (2.8) and (2.9) we obtain the required system of gas dynamic equations, which may be written as follows:

$$\frac{\partial n_a}{\partial t} = \frac{\partial}{\partial z}\left[\frac{\chi_a}{T_a}\sum_{n=1}^{3}\beta_a^{(n)}P_a^{(n)}\right] \tag{2.21a}$$

$$\frac{\partial n_a T_a}{\partial t} = \frac{2}{3}\frac{\partial}{\partial z}\left[\chi_a\sum_{n=1}^{3}\gamma_a^{(n)}P_a^{(n)}\right] \mp$$

$$\mp \frac{2}{3}\chi_a P_a^{(1)}\sum_{n=1}^{3}\beta_a^{(n)}P_a^{(n)} \pm n\frac{T_e - T_i}{\tau}$$

where

$$\tau = \frac{3}{16}\sqrt{\frac{2}{\pi}}\frac{m_i T_e^{3/2}}{\Lambda e^4 m_e^{1/2} n}$$

The term $n(T_e - T_i)/\tau$ on the right-hand side of Eq. (2.21b) describes the heat exchange between electrons and ions. The upper signs in formula (2.21b) relate to ions and the lower ones to electrons. Here and below we omit the averaging bar above the values E, n_a, T_a, $P_a^{(n)}$.

The characteristics of the corrugated magnetic field are represented in the above system of equations by the integral

$$I = \frac{H_{\max}}{l}\int_{s_1}^{s_2}\frac{ds}{H(s)} \tag{2.22}$$

on which the coefficient χ_a depends (see expression (2.20)). The effect of the corrugation on mass and energy transfer increases as I. With a fixed mirror ratio the integral I depends only on the magnetic field profile and increases when the length of the mirror l_m decreases in relation to the length of the homogeneous magnetic field region. When $l_m \to 0$ ("point" mirrors) I attains its maximum value, $I = k$. For practical purposes the formula $I = k$ can be used when $l_m \lesssim l/k$.

2.3 Analysis of the Macroscopic Equations

We now consider the practical application of the expansion of a plasmoid into a vacuum. Here the quasi-neutrality condition $n_e = n_i = n$ also means that the current in

the plasma is zero, i.e. $q_e = q_i$. Determining the electric field from this relation and substituting it in expressions (2.21a) and (2.21b) we obtain a system of three equations for n, T_e and T_i:

$$\frac{\partial n}{\partial t} = \frac{\partial}{\partial z}\left\{\frac{\chi_i}{T_i} \times \left[0.45\left(\frac{T_e}{T_i}+1\right)\frac{\partial \ln n}{\partial z} + 1.10\frac{T_e}{T_i}\frac{\partial \ln T_e}{\partial z} + 1.06\frac{\partial \ln T_i}{\partial z}\right]\right\} \tag{2.23}$$

$$\begin{aligned}\frac{\partial n T_e}{\partial t} = {} & \frac{\partial}{\partial z}\left[\chi_e \frac{\partial}{\partial z}(0.55\ln T_e)\right] \\ & + \left[\chi_i \frac{\partial}{\partial z}(0.66\ln n + 1.62\ln T_e)\right] \\ & \times \frac{T_e}{T_i} \times \left[0.45\left(\frac{T_e}{T_i}+1\right)\frac{\partial \ln n}{\partial z} + 1.10\frac{T_e}{T_i}\frac{\partial \ln T_e}{\partial z} + 1.06\frac{\partial \ln T_i}{\partial z}\right] - n\frac{T_e - T_i}{\tau}\end{aligned} \tag{2.24}$$

$$\begin{aligned}\frac{\partial n T_i}{\partial t} = {} & \frac{\partial}{\partial z}\left\{\chi_i \times \left[1.16\left(\frac{T_e}{T_i}+1\right)\frac{\partial \ln n}{\partial z} + 2.82\frac{T_e}{T_i}\frac{\partial \ln T_e}{\partial z} + 3.91\frac{\partial \ln T_i}{\partial z}\right]\right\} \\ & - \left[\frac{\chi_i T_e}{T_i}\frac{\partial}{\partial z}(0.66\ln n + 1.62\ln T_e)\right] \\ & \times \left[0.45\left(\frac{T_e}{T_i}+1\right)\frac{\partial \ln n}{\partial z} + 1.10\frac{T_e}{T_i}\frac{\partial \ln T_e}{\partial z} + 1.06\frac{\partial \ln T_i}{\partial z}\right] + \frac{T_e - T_i}{\tau}\end{aligned} \tag{2.25}$$

(wherever possible, we have neglected terms of the order of $\sqrt{m_e/m_i}$).

Equations (2.23–2.25) conserve the number of particles and their total energy:

$$\int n dz = \int n_0 dz \tag{2.26}$$

$$\int n(T_e + T_i)dz = \int n_0(T_{e0} + T_{i0})dz \tag{2.27}$$

(n_0, T_{e0}, and T_{i0} denote the initial values of the respective parameters).

It will be seen from expression (2.23) that the characteristic plasmoid expansion time (i.e. the density variation time) is equal in order of magnitude to $t_1 \sim I^2 L^2/\lambda v_{Ti}$. The electron temperature equalization time along the plasmoid is much less: $t_2 \sim I^2 L^2/\lambda v_{Te} \sim t_1\sqrt{m_e/m_i}$. This means that the electron temperature is uniform along the plasmoid: $\partial T_e/\partial z = 0$. The ion temperature, generally speaking, is not equalized along the plasmoid because ion thermal conductivity is low. But in the case of practical interest where $L > (\lambda/I)(m_i/m_e)^{1/4}$ the electron-ion energy exchange time is small compared with t_1 and the equality $T_i \simeq T_e = T(\partial T/\partial z = 0)$ is accordingly fulfilled. Hence energy integral (2.27) can be written as

$$T\int n dz = \text{const}$$

But since the number of particles is also conserved (see expression (2.26), the latter equality means that T is also independent of time.

Thus the motion of sufficiently long ($L > (\lambda/I) \times (m_i/m_e)^{1/4}$) plasmoids can be described by the single equation (2.28) which is also considerably simplified in view of the condition $\partial T/\partial z = 0$

$$\frac{\partial n}{\partial t} = \zeta \frac{\partial^2 \ln n}{\partial z^2}, \qquad \zeta = \frac{0.91\, T^{5/2}}{m_i^{1/2} I^2 \Lambda e^4} \tag{2.28}$$

For reference purposes we may show one of the exact solutions of this equation, corresponding to an initial condition of the form

$$n = n_0 \left(1 + \frac{z^2}{d_0^2}\right)^{-1}$$

For constant ζ (uniform corrugation) this solution is

$$n = \frac{d_0 n_0}{d} \left(1 + \frac{z^2}{d^2}\right)^{-1}$$

where

$$d = d_0 + \frac{2\zeta t}{d_0 n_0}$$

Let us now consider these results in relation to the problem of thermal insulation of a plasma in a device of finite length. If the plasma is in contact with the ends, its cooling time is $t_2 \sim I^2 L^2 / \lambda v_{Te}$, where L is the length of the devices. On the other hand, the characteristic expansion time for a plasmoid of length L is $t_1 \sim (m_i/m_e)^{1/2} t_2$. Therefore it might be thought that the plasma thermal insulation time could be increased to values of $\sim t_1$, by establishing a plasmoid of length $\sim L/2$ in the center of the device. Then the presence of plasma-free gaps between the ends of the device and the edges of the plasmoid would prevent heat transfer to the ends. In fact, however, immediately after the plasmoid is created its boundary layers, which have a thickness of the order of the effective free-path length (i.e. λ/I), begin to expand freely into the vacuum from both ends of the plasmoid at a rate of $\sim v_{Ti}$ and arrive at the ends of the device in the time $\sim L/v_{Ti}$. The plasma density between the plasmoid and the ends of

the device reaches $n_0(\lambda/IL)$ and continues to increase. This means that the effective free-path length in the region between the plasmoid and the ends will not be greater than L, so that heat transfer in this region can be described, at least qualitatively, by the macroscopic equation (2.24). From this equation it will be seen that the plasma thermal conductivity coefficient is independent of the density. However, this means that the plasma cooling time will be of the same order as when the plasma fills the whole space between the mirrors from the very beginning.

The phenomenon just described (which may be termed the "precursor effect") is significant only in conditions where the plasma breaking away from the plasmoid boundaries accumulates between the plasmoid and the ends of the device. If the boundary conditions corresponding to leakage of a plasma into a vacuum are fulfilled at the ends, the confinement time of the hot plasma inside the device will be of the order of t_1. This condition can be provided, for example, by means of regions at the ends of the device which have strongly expanding force lines.

Let us now consider, briefly, the problem of distortion of the magnetic field by the plasma. This question is of great importance for the pulsed reactor concept since this system, as was mentioned in the introduction, is expected to operate with $\beta \gg 1$. In this "wall" confinement regime the magnetic field suppresses only transverse thermal conductivity but the equilibrium in this direction is provided by the rigid walls. The distortions of the magnetic field with $\beta \gg 1$ result from both radial and axial plasma flow. The first effect was studied in a number of paper [25–27]. These papers are mainly devoted to the analysis of efficiency of thermal conductivity suppression. They are based on the model of an infinitively long solenoid with straight magnetic

field. Without discussing here the results related to the efficiency of radial thermal isolation let us consider the main features of the magnetic field evolution. If the conductivity of the wall is high enough, the plasma heating does not lead to a noticeable decrease of the magnetic field in the center of the machine (see, for example [26]). This result shows that predictions in [28] of complete expulsion of magnetic field from the central part to a thin layer near the wall are not valid.

A more advanced model of the solenoid, with a corrugated magnetic field but plasma parameters still periodic in the axial direction (without an average pressure gradient) was studied in [29]. It was found that, if the wall is a good conductor and if it has a form close to one of the magnetic surfaces, then magnetic flux conservation prevents noticeable deformation of the magnetic configuration; the mirror ratio increases a little near the axis and is not strongly decreased on the periphery. Note that if the wall is a sufficiently good conductor, a magnetic surface will automatically conform to it. By corrugating the wall it is possible to create practically any magnetic field profile along the axis of the system.

If one uses a well conducting corrugated wall the longitudinal pressure gradient and plasma axial flow caused by it can not lead to substantial distortion of the corrugated magnetic surfaces. In fact, the perturbation of magnetic field results not from the absolute value of pressure but from its axial gradient. Since the pressure difference along one mirror trap is small $\Delta p \sim pl/L$, then the minimum of the magnetic field strength needed for multiple mirror confinement is determined by the inequality:

$$H^2/8\pi \geq hTl/L$$

One can see that for the case of sufficiently long plasma bunches plasma flow does not result in a strong limitation on β ($\beta \leq L/l$). A derivation of this criterion is given in [12].

Finally, we mention an interesting possibility for the case of strong magnetic field ($\beta \ll 1$), for which the plasma is magnetically confined. Then, if a traveling multiple mirror field moving from the plasma ends toward the center can be constructed, one can obtain a steady state axial confinement [20]. If $l \ll \lambda/k$, then confinement theory predicts a steady state length of the plasma bunch of the order of

$$L = \lambda v_{Ti}/k^2 u_0$$

where u_0 is the velocity of the field motion. This estimate is valid only if $L \gg \lambda/k$, and, as we shall see in the concluding section, gives only a rough approximation to the complete dynamics. The idea has also been considered as a method of improving steady-state confinement [30].

2.4 Plasma Diffusion Along A Weakly Corrugated Magnetic Field with with Small-Scale Corrugation

A qualitative consideration of the plasma flow along a weakly corrugated magnetic field was carried out in Section 1. The flow was classified into three different regimes of plasma motion (see Fig. 2). This subsection, based on paper [21], is devoted to a quantitative description of the small-scale limiting case (1.5), when the trapped particles execute several oscillations from mirror to mirror before they become untrapped.

In both its physical sense and calculation procedure this regime is quite analogous to the problem of collisional damping of a finite-amplitude electrostatic Langmuir wave [23]. Because of their similarity we will limit ourself with only a brief description of the scheme of calculation and will concentrate attention on these features which are inherent in considering the problem for the magnetic field case.

To derive the axial transport equation for the case of a weakly corrugated magnetic field it is more convenient to use a somewhat different approach than that in Section 2.1. It is based on finding an average, over one mirror cell, of the friction force caused by the interaction between the particles and magnetic field. To calculate this, it is necessary to know the ion distribution function. Under the same assumptions as in Section 2.1 the kinetic equation for the ion component has the form

$$\frac{\partial F_i}{\partial t} + v\cos\theta\frac{\partial F_i}{\partial s} + \frac{v\sin\theta}{\partial H}\frac{\partial H}{\partial s}\frac{\partial F_i}{\partial \theta} = St_{ii}. \tag{2.29}$$

For simplicity we have cancelled the term containing the electric field from the left side of (2.1) that can be taken into account directly in the final equations.

Integrating (2.29) over the velocities with weight $m_i v\cos\theta$ and averaging with weight $1/H$ over the single mirror cell one gets the expression for the frictional force:

$$F_{fr} = -\frac{H_{\max}}{Il}\int_{s_1}^{s_2}\frac{ds}{H^2}\frac{dH}{ds}\int\frac{m_i v^2}{2}\sin\theta F_i d^3v \tag{2.30}$$

It follows from (2.30) that F_{fr} is governed by that part of correction f_i to a Maxwellian distribution which is symmetric with respect to $\cos\theta$ and is an odd function of s. This correction f_i is the first term of an expansion of the distribution function F_i in a power of the small parameter $\lambda/(k-1)^{1/2}L \ll 1$ (see (1.6)). It is localized in velocity

space on a scale of the order of a few $\Delta\theta$ (1.4) near the value $\theta = \pi/2$. Since this part of the velocity space is very narrow one can simplify the collision term for f_i using the same arguments as in Section 2.1. After this operation the kinetic equation for f_i takes the form

$$v\cos\theta\frac{\partial f}{\partial s} + \frac{v\sin\theta}{2H}\frac{\partial H}{\partial s}\frac{\partial f}{\partial\theta} = \frac{\nu_i\alpha_i}{\sin\theta}\frac{\partial}{\partial\theta}\sin\theta\frac{\partial f}{\partial\theta}. \tag{2.31}$$

where $\nu_i = 2\pi\Lambda e^4 n/m_i^2 v^3$, and $\alpha_i(v)$ is given in Section 2.1. The term $\partial f_i/\partial t$ is omitted as it is second order with respect to the small parameter (1.6), that corresponds to a very slow plasma expansion along a magnetic field.

The factor $\alpha_i(v)$ describes the effect of collision between trapped particles and Maxwellian ones. In paper [23] where the collision damping of a Langmuir wave with a high phase velocity was considered, the relative velocities of these two groups of the particles were much greater than the thermal velocities and correspondingly an asymptotic $\alpha_i(v) = \text{const}$ was used. In the present context the directional plasma velocity which plays the role of the phase velocity is small compared with the thermal one. For this reason the formal use of the results obtained in [23] for the calculation of the frictional force between plasma and magnetic field resulted in a wrong numerical coefficient for F_{fr} in [31].

The Eq. (2.31) for f_i can be solved by expanding in powers of another small parameter (1.5) in accordance with the scheme described in Section 2.2. Under the integration of the system of equations for r_i and p_i the general boundary condition (2.11) that makes them periodic is used. Two additional boundary conditions in velocity space are applied to find r_i. One of them was already used in Section 2.2 and

corresponds to the vanishing of r_i at the transit-trapped particle boundary (i.e. when $\varepsilon = \mu H_{max}$). Another one provides conversion of F_i into a shifted Maxwell distribution in the region of transiting particles far from the boundary with trapped particles, that is:

$$r_i \rightarrow F_{Mi} \frac{m_i v u}{T} \cos\theta$$

when $k - 1 \ll 1 - \mu H_{max}/\varepsilon \ll 1$. The solution for r_i which satisfies these conditions has a form

$$r_i = \begin{cases} r_0(\varepsilon) \int_{\varepsilon/H_{max}}^{\mu} \frac{d\mu'}{\mu'} \left[\int_{s_1}^{s_2} (\varepsilon - \mu' H)^{1/2} ds \right]^{-1} & \mu < \varepsilon/H_{max} \\ 0 & \mu > \varepsilon/H_{max} \end{cases} \qquad (2.32)$$

where $r_0(\varepsilon) = -F_{Mi}(\varepsilon)(m_i \cdot 2)^{1/2}(\varepsilon l u/T)$. If r_i is known, the even function of $\cos\theta$, p_i, can be determined by integrating (2.16) over s.

$$p_i = p_0(\varepsilon) \frac{\partial}{\partial \mu} \left[\int_{s_1}^{s} (\varepsilon - \mu H)^{1/2} ds \Big/ \int_{s_1}^{s_2} (\varepsilon - \mu H)^{1/2} ds \right] \qquad (2.33)$$

where $p_0(\varepsilon) = -2\varepsilon u l \nu_i \alpha_i m_i F_{Mi}/TH$.

In variables ε, μ the expression (2.30) has a form:

$$F_{fr} = -\pi \left(\frac{2}{m} \right)^{3/2} \int_{s_1}^{s_2} \frac{ds}{H} \frac{dH}{ds} \int_0^{\infty} d\varepsilon \int_0^{\varepsilon/H} \frac{\mu d\mu p_i}{(\varepsilon - \mu H)^{1/2}} \qquad (2.34)$$

In calculating F_{fr} we should break up the integral over μ into three parts: over the phase space corresponding to trapped particles, untrapped particles and the narrow transition layer which arises near the boundary $\mu = \varepsilon/H_{max}$ because of Coulomb

collisions. Since the collisions result in diffusion of the particles in velocity space, the width $\delta\mu$ of this layer can be easily estimated as follows:

$$\delta\mu \, H_{max}/\varepsilon \simeq l/\lambda(k - 1)^{1/2}$$

In this layer the solutions given above are not valid. In calculating the fluxes q_a and Q_a in Section 2.2 it was of no importance, since the contributions to the corresponding integrals from the transition layer were small in comparison with the contribution from the transiting particles. In calculating (2.34) the situation changes and contributions from the transiting particles and from the layer are quite comparable while the contribution from trapped particles is negligibly small.

Although the function p_i is unknown in the transition layer the contribution from it in (2.34) can be calculated by the standard method of integrating the exact equation (2.16) across the layer. Since the layer is narrow, the coefficients in (2.34) can be considered as constants over the integration. So finally the integral through the transition layer is expressed by the derivative $\partial r_i/\partial\mu$ outside of the layer where it is described by expression (2.32). This operation allows the contribution of the transition layer to be taken into account in an explicit form.

In the final expression for F_{fr} the integral of $\alpha_i(\varepsilon)$ over ε is calculated analytically. The integration over the variables μ and s leads to integrals that can be found for a specific dependence $H(s)$. As an example we adopt a field with a sinusoidal profile

$$H(s) = H_{min} + (H_{max} - H_{min}) \sin^2 \frac{\pi s}{l} \qquad (2.35)$$

then the integral becomes an elliptic integral of the second kind, the numerical value

of which gives

$$F_{fr} = -1.82 \frac{h_2 m_i^{1/2} \Lambda e^4}{T_i^{3/2}} u(k-1)^{1/2} \tag{2.36}$$

A somewhat more detailed description of this calculation can be found in [32].

Using (2.36) one can derive axial transport equations in a weakly corrugated magnetic field. To illustrate this approach we use the diffusive plasma equation for the case, when $T_e = T_i = T$ and $\partial T/\partial z = 0$. The velocity of plasma expansion is determined by the balance of the forces acting on an ion component.

$$e\, n\, E_{\parallel} - \frac{\partial p_i}{\partial z} + F_{fr} = 0 \tag{2.37}$$

Since the frictional force for the electron component is negligibly small, the electric field can be written as follows: $enE_{\parallel} = -\partial p_e/\partial z$. Finding the expansion velocity from (2.37) and substituting it in the equation of mass conservation, one obtains the diffusive equation for the plasma density:

$$\frac{\partial n}{\partial t} = \frac{\partial}{\partial z} D \frac{\partial n}{\partial z}, \tag{2.38}$$

$$l(k-1)^{-3/2} \ll \lambda \ll L(k-1)^{1/2}$$

where

$$D = \frac{1.1\, T^{5/2}}{n\, m_i^{1/2} \Lambda e^4 (k-1)^{1/2}}.$$

The inequalities in (2.38) provide the conditions for small-scale corrugation and the smallness of the expansion velocity $u \sim D/L$ in comparison with the ion thermal velocity.

3. PLASMA DYNAMICS WITH LARGE-SCALE CORRUGATION

As already defined in Section 1, the large-scale corrugation regime corresponds to a regime when the mean free path is sufficiently small in comparison with the characteristic space scale of the magnetic field that the plasma obeys the ordinary two-fluid gas dynamic equations. The method of reduction of these equations in an application to the case of slow plasma expansion developed in [12] is described in Section 3.1. Note that a few years after [12] the derivation of the same equations was independently carried out in [33, 34]. While the results in [33] did not coincide exactly with those in [12], in the subsequent paper [34] equations were obtained which were identical with the results of [12].

A maximum efficiency of multiple mirror confinement and a saving of the energy consumption required to maintain the magnetic field is achieved in multiple mirror fields with "point" mirrors, whose length l_m is much less that the corrugation period l. In this two scale field there is an intermediate range of (1.10) which is between the cases of small-scale and large-scale corrugation. The plasma confinement theory developed in [35] for this interval of parameters is described in Section 3.2. Approximately at the same time, independently from [35], some results, concerned with this case, were published in [22]. In distinction from [35], the effects of ambipolar potential and temperature gradients were not taken into account so the results of [22], related to this regime, were more qualitative. The ambipolar effects were taken into consideration by the authors later in [36]. Both in [22] and in [36] the results were extended to the important regime of $\lambda \sim l$, a regime not treated in [35].

In accordance with the classification of Section 1, in the case of weakly modulated magnetic field there is also an intermediate regime ("plateau" regime) which is between the cases of small-scale and large-scale corrugation. In Section 3.3 the derivation of the frictional force based on [21] is described. The theoretical results are extended to parameters which were realized in some multiple mirror experiments [37].

The idea of increasing the Coulomb collision frequency by means of inserting a plasma small amount of heavy impurities with $z \gg 1$ was suggested long ago (see, for example, [38]). The possibility of improvingthe efficiency of multiple mirror confinement was pointed out in [39] and was studied in detail in [40–42]. As developed in these papers, the quantitative theoretical description of the impurity dynamics in a multiple mirror magnetic field is discussed in Section 3.4.

3.1 The Description of a Plasma Motion with Two-Fluid Gas Dynamic Equations

When $\lambda \ll l \ll L$ plasma behavior can be described from the outset with double-fluid gas-dynamic equations. To obtain the equations describing slow ($u \ll v_{Ti}$) expansion of the plasma, we use the same method as in Section 2; first, by studying plasma flow inside an individual magnetic mirror cell we find the mass and energy fluxes and then, substituting these in the conservation laws of the type (2.8) and (2.9), we obtain a closed system of equations for slow processes.

For solving the first part of the problem the motion inside each cell can be regarded as steady-state, because all the parameters of the problem vary with a characteristic time L/u, which is much greater than the time l/u determining the passage of the plasma through a cell. A further simplification is associated with the fact that over

the length of one cell there is little variation in any of the plasma parameters: $\Delta n = n(s_2) - n(s_1) \ll n$, $\Delta T_a = T_a(s_2) - T_a(s_1) \ll T_a$, and so on. Thus only first order terms with respect to Δn and ΔT_a need to be retained in the gas dynamics equations. Since our main practical interest here is expansion of the plasma, we shall consider the macroscopic electron and ion velocities to be equal from the very outset: $u_e = u_i = u$.

We shall project a system of double-fluid gas dynamic equations onto a line of force. As a result, taking the above points into consideration, we find that

$$-n\frac{\partial T_a}{\partial s} - T_a\frac{\partial n}{\partial s} \mp R \pm e\,n\,E_{\parallel} + \frac{4\eta_a}{3}\frac{H^{3/2}}{\bar{n}}\frac{\partial}{\partial s}H^{-2}\frac{\partial}{\partial s}(qH^{1/2}) = 0 \tag{3.1}$$

$$\frac{\partial}{\partial s}\frac{q}{H} = 0 \tag{3.2}$$

$$\frac{\partial}{\partial s}\frac{Q_a}{H} = 0 \tag{3.3}$$

where $q = nu$ is the mass flux, $Q_a = -\kappa_a(\partial T_a/\partial s) + (5/2)q\,T_a$ is the energy flux, $R = -0.71\,n\,(\partial T_e/\partial s)$ is the thermal force and η_a and κ_a are the longitudinal viscosity and thermal conductivity determined by the relations [2]*

$$\eta_i = 0.404\frac{m_i^{1/2}T_i^{5/2}}{\Lambda e^4} \qquad \kappa_i = 4.04\frac{\eta_i}{m_i}$$

$$\eta_e = 0.215\frac{m_e^{1/2}T_e^{5/2}}{\Lambda e^4} \qquad \kappa_e = 4.33\frac{\eta_e}{m_e}$$

The upper sign in equation (3.1) relates to ions and the lower one to electrons. It

*To avoid misunderstandings, we would point out that our notation differs slightly from that used by Braginsky [18].

should be noted that when $l > \lambda(L/\lambda)^{1/3}$ the equation for ion movement must include an inertial term, $m_i\, nu\, \partial u/\partial s$. However, this term does not affect the expressions for q and Q_a given below.

The quantities q and Q_a can be found from the given values of ΔT_a and Δn using Eqs. (3.1)–(3.3):

$$q = \frac{-H}{I_1 H_{\max}} \frac{l^2 n \dfrac{\partial}{\partial z} n (T_e + T_i)}{\eta_i} \tag{3.4}$$

$$Q_a = \frac{5}{2} q T_a - \frac{H}{I_2 H_{\max}} \kappa_a \frac{\partial T}{\partial z} \tag{3.5}$$

Here

$$I_1 = \frac{3l}{H_{\max}} \int_{s_1}^{s_2} \frac{ds}{H} \left[\frac{\partial H}{\partial s}\right]^2, \quad I_2 = \frac{1}{l H_{\max}} \int_{s_1}^{s_2} H ds$$

The derivatives $\partial/\partial z$ in expressions (3.4) and (3.5) are introduced as in expression (8). The averaging bars above n and T_a are omitted. In deriving relations (3.4) and (3.5) we neglected the electron viscosity (since it is much smaller than the ion viscosity) and, in addition, excluded the electric field with the aid of the equation for electron dynamics

$$enE_{\parallel} - R = -n \frac{\partial T_e}{\partial s} - T_e \frac{\partial n}{\partial s} \tag{3.6}$$

The law of conservation of matter in gas dynamics coincides precisely with expression (2.8). Substituting in that equation the expression obtained above for q, we find the equation for n:

$$\frac{\partial n}{\partial t} = \frac{l^2}{II_1} \frac{\partial}{\partial z} \frac{n}{\eta_i} \frac{\partial}{\partial z} [n(T_e + T_i)] \tag{3.7}$$

The gas dynamic energy conservation law is written as follows [18]:

$$\frac{\partial n T_a}{\partial t} + \frac{2}{3I} \frac{\partial Q_a}{\partial z} \mp \frac{2 H_{\max}}{3II} \int_{s_1}^{s^2} \frac{\left[e E_{\parallel} - \dfrac{R}{n}\right] q(s) ds}{H(s)} = 0 \tag{3.8}$$

Substituting relations (3.5) and (3.6), we find the equations for T_e and T_i:

$$\begin{aligned} \frac{\partial n T_a}{\partial t} = {} & \frac{2}{3I} \frac{\partial}{\partial z} \left[\frac{\kappa_a}{I_2} \frac{\partial T_a}{\partial z} + \frac{5}{2} \frac{^2 n T_a}{I_1 \eta_i} \frac{\partial}{\partial z} n(T_e + T_i)\right] \\ & \pm \frac{2l^2}{3II_1\eta_i} \left[\frac{\partial}{\partial z} n(T_e + T_i)\right] \left[\frac{\partial}{\partial z} n T_e\right] \pm n \frac{T_e - T_i}{\tau} \end{aligned} \tag{3.9}$$

To illustrate the results obtained, let us consider the motion of a plasmoid when $\lambda > l(I_2/I_1)^{1/2}(m_e/m_i)^{1/4}$ and $L > l(II_1)^{-1/2}(\ _i/m_e)^{1/4}$. The first of these conditions indicates that the electron thermal conductivity provides uniform T_e along the plasmoid, and the second that heat exchange between electrons and ions maintains $T_i = T_e = T$. Considerations similar to those in Section 2 show that T is then independent not only of the coordinates but also of time. The system of gas-dynamic equations then resolves into a single equation for the density

$$\frac{\partial n}{\partial t} = \xi \frac{\partial}{\partial z} n \frac{\partial n}{\partial z}, \quad \xi = \frac{2Tl^2}{\eta_i II_1} \tag{3.10}$$

With the initial condition

$$n|_{t=0} = \begin{cases} n_0 \left[1 - \dfrac{z^2}{d_0^2}\right], & |z| < d_0 \\ 0 & |z| > d_0 \end{cases}$$

this equation has the solution

$$n = \begin{cases} \dfrac{n_0 d_0}{d}\left[1 - \dfrac{z^2}{d_0^2}\right], & |z| < d \\ 0 & |z| > d \end{cases}$$

where

$$d = (6\, d_0 n_0 \xi t)^{1/3}$$

The effect of the magnetic field profile on the plasma expansion rate is represented in Eq (3.10) by the product H_1. This quantity can be calculated for quite general magnetic field configurations in which the mirror scale length l_m is uncoupled from the cell length l, as shown in Fig. 3. For example, if the function $H(s)$ takes the form shown in Fig. 4, H_1 is equal to

$$\frac{6l}{l_m}(k-1)\ln k\left[1 + 2\frac{l_m}{l}\left(\frac{\ln k}{k-1} - 1\right)\right]$$

If $k \gg 1$ and $l_m \ll l$, then $H_1 \simeq 6(l/l_m)k \ln k$. The plasma expansion rate is then of the order of $v_{Ti}\, l\, l_m/(\lambda L\, k\, \ln k)$.

The validity condition for the gas dynamic approximation $\lambda(\partial \ln u/\partial s) \ll 1$ in the case of the magnetic field shown in Fig. 4 may be written in the form $\lambda \ll l_m$. Thus, between the zones of validity of the results in Section 2 ($l < \lambda/k$) and the results in this section ($l > l_m > \lambda$) there is a region $l_m < \lambda < kl$ where none of these results is valid. A kinetic approach is called for in the mirror region, and double-fluid gas dynamics in the rest of the cell. Based on the results of paper [35] we now describe this intermediate parameter range.

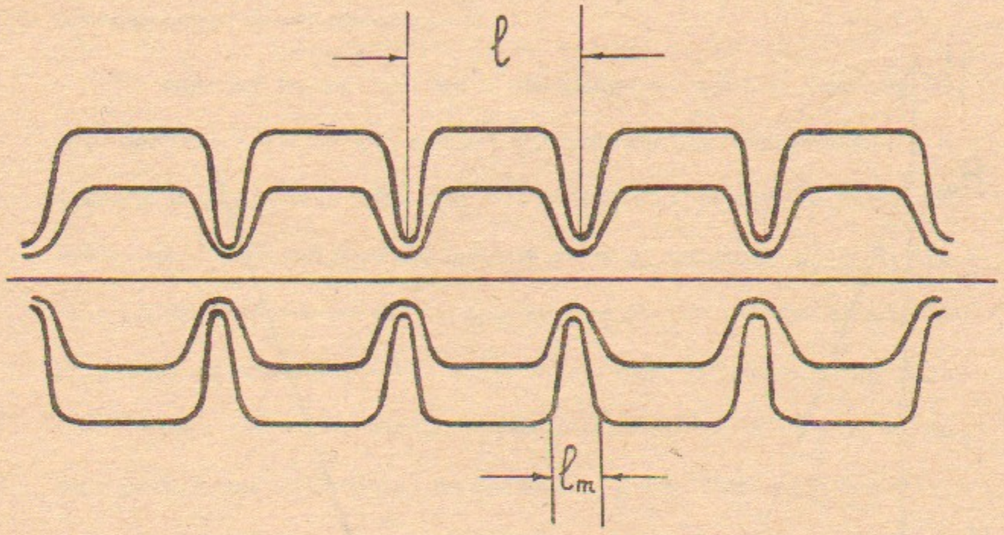

Figure 3. Geometry of the force lines for a magnetic field configuration in which the mirror scale length l_m is much less than the cell length.

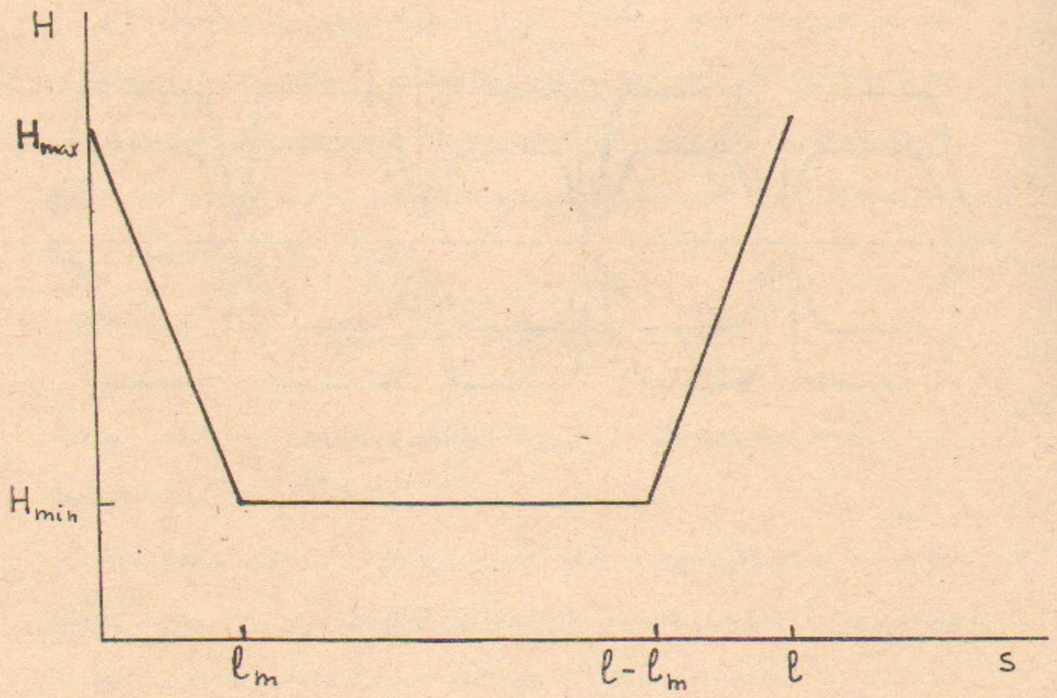

Figure 4. An approximate form for the magnetic field strength, which is useful for calculations.

3.2 The Intermediate Regime in a Multiple-Mirror Field with "Point" Mirrors

Since in the range of mean free paths $l_m \ll \lambda$ the dynamics of the plasma expansion should not depend on the size and shape of a mirror, we will solve the problem in the approximation that $l_m \cong 0$ and the field in the space between mirrors is uniform (the square magnetic well approximation).

The procedure for the derivation of the gasdynamic equations describing the dispersion along a field tube of a plasmoid with a characteristic longitudinal scale L is analogous to the system of calculations used in Section 2.1. First one must solve the steady-state problem and relate the fluxes of matter q_a and energy Q_a of the two plasma components with the drops in concentrations Δn_a and temperatures ΔT_a and the potential $\Delta\phi$ between the centers of two adjacent mirror cells. At this stage of the calculation one must assume that the differences Δn_a, ΔT_a, and $\Delta\phi$ are given and do not depend on time. We introduce the coordinates along the field tube in such a way that a mirror separating two mirror cells is located at the point $s = 0$. Then

$$\begin{aligned} \Delta n_a &= n_a(l/2) - n_a(-l/2) \\ \Delta T_a &= T_a(l/2) - T_a(-l/2) \\ \Delta\phi &= \phi(l/2) - \phi(-l/2) \end{aligned} \tag{3.11}$$

We assume that the plasma bunch is sufficiently extended and occupies a large number of mirror cells ($N \simeq L/l \gg 1$). In this case the values of n_a, T_a, and ϕ vary only slightly on the scale of a single mirror cell ($\Delta n_a \ll n_a$, $\Delta T_a \ll T_a$). The nature of their variation is different in different sections of a field tube; within the mirror cell where the flow has a collisional nature the parameters n_a, T_a, and ϕ vary smoothly in

accordance with the equations of two-fluid hydrodynamics. In the region of a mirror the hydrodynamic approximation breaks down. Here the plasma parameters can undergo sharp jumps whose spatial scale is on the order of the size of the mirror. Therefore, in a solution of the problem in zero order with respect to l_m/λ one must take into account the fact that the boundary values of n_a, T_a, and ϕ may not coincide to the left and to the right of the mirror. We determine the jumps in these values upon the transition through a mirror by the equalities

$$\delta n_a = n_a(+0) - n_a(-0),\ \delta T_a = T_a(+0) - T_a(-0)$$
$$\delta\phi = \phi(+0) - \phi(-0) \tag{3.12}$$

For further calculations we will use the assumption that the mirror ratio is large ($k \gg 1$). This assumption allows us to find, in explicit form, the connection between the fluxes of matter and energy, and the values (3.12). Let us examine the flow of any component of the plasma through a mirror. If the mirror ratio were equal to infinity, then the exchange of particles between mirror cells would be absent and a Maxwellian velocity distribution with parameters corresponding to the given mirror cell would be established within each of them. With a finite mirror ratio the Maxwellian distribution near a mirror is disturbed by the flux of particles from the next mirror cell which has different values of the parameters (concentration, temperature, and potential). The disturbance in the distribution function is proportional to the difference in the values of the parameters and also, since the mirror ratio is large, to the smallness of the number of particles, $\sim n/k$, penetrating from mirror cell to mirror cell

$$F(v) - F_M(v) = f(v) \sim \frac{1}{k}\,\frac{\Delta n}{n}$$

In the calculation of the fluxes of matter and energy the contribution to the integral from the function $F(v)$ gives a narrow region of phase space $v_\perp{}^2/v^2 = \sin^2\theta \le 1/k$. Keeping this in mind, one can verify that the allowance for a disturbance $f(v)$ would lead to the appearance of terms containing the small value k^{-1} in the equations for the fluxes. Therefore, the fluxes of matter and energy can be calculated with an accuracy of the terms of order k^{-1} by assuming that the distribution functions near a mirror are Maxwellian. The results of these calculations performed in a linear approximation with respect to δn_a, δT_a, and $\delta\phi$ have the form

$$q_a = -\frac{n_a}{k}\left(\frac{T_a}{2\pi m_a}\right)^{1/2}\left[\frac{\delta n_a}{n_a} + \frac{1}{2}\,\frac{\delta T_a}{T_a} \pm \frac{e\,\delta\phi}{T_a}\right] \tag{3.13}$$
$$Q_a = -\frac{n_a T_a}{k}\left(\frac{T_a}{2\pi m_a}\right)^{1/2}\left[2\,\frac{\delta n_a}{n_a} + 3\,\frac{\delta T_a}{T_a} \pm 2\,\frac{e\,\delta\phi}{T_a}\right]$$

In the mode when the plasma bunch expands freely the condition of quasineutrality is expressed by the equality $q_e = q_i \equiv q$, which allows one to eliminate from (3.13) the jump in potential at a mirror. Equations (5) take the form

$$q = -\frac{1}{k(2\pi m_i T_i)^{1/2}}\left[(T_e + T_i)\delta n + \frac{n}{2}(\delta T_e + \delta T_i)\right]$$
$$Q_e = -\frac{n}{k}\left(\frac{2T_e}{\pi m_e}\right)^{1/2}\delta T_e \tag{3.14}$$
$$Q_i = -\frac{1}{k}\left(\frac{T_i}{2\pi m_i}\right)^{1/2}\left[2(T_e + T_i)\delta n + 3n\,\delta T_i + n\,\delta T_e\right]$$

Terms containing the small value m_e/m_i are omitted in Eqs. (3.14)

Now we can find the connections between the jumps at a mirror, which figure in (3.14), and the assigned drops in the parameters (3.11) between adjacent mirror cells.

The transition from free flow at the mirrors to hydrodynamic flow in the central section of a mirror cell takes place near a mirror at distances on the order of the effective mean free path. We can take the effective mean free path as the distance $\lambda_{eff} \simeq \lambda/k$ in which a transiting particle is scattered through an angle $\Delta^2 \simeq k^{-1}$ and enters the region of phase space occupied by trapped particles. If $\lambda_{eff} \ll l$, then the equations of two-fluid hydrodynamics can be used everywhere within the mirror cells to describe the plasma flow [18].

We can join the steady-state solutions for the regions of Knudsen and hydrodynamic flows by using the fact that the fluxes of matter and energy are nearly constant along a flux tube. The variations in these values along the length of a mirror cell are quantities of the second order of smallness with respect to the parameter l/L, whereas the fluxes are values of the first order of smallness. By equating the hydrodynamic equations for the fluxes of matter and energy with the values of (3.14) we obtain equations describing the temperature distributions in the hydrodynamic region:

$$-\chi_a \frac{\partial T_a}{\partial s} + \frac{5}{2} q T_a = Q_a \tag{3.15}$$

The thermal-conductivity coefficients are given by the equations

$$\chi_i = 1.63 \frac{T_i^{5/2}}{\Lambda e^4 m_i^{1/2}}, \qquad \chi_e = 0.93 \frac{T_e^{5/2}}{\Lambda e^4 m_e^{1/2}}$$

These equations must be supplemented by the condition of the steady-state flow. Neglecting viscosity, it is just the requirement of constancy of the total pressure along a field tube

$$\frac{\partial}{\partial s} n(T_e + T_i) = 0 \tag{3.16}$$

We integrate Eqs. (3.15) and (3.16) with respect to s between the centers of the mirror cells (from the point $s = -l/2$ to $s = l/2$), excluding a region of width δ ($\lambda_{eff} \ll \delta \ll l$) on both sides of the mirror where the hydrodynamic approximation breaks down. As a result we obtain

$$\begin{gathered} \frac{x_a}{l}[\Delta T_a - T_a(\delta) + T_a(-\delta)] = Q_a - \frac{5}{2} q T_a \\ n(\Delta T_e + \Delta T_i) + (T_e + T_i)\Delta n = (T_e + T_i)[n(\delta) - n(-\delta)] \\ + n[T_e(\delta) - T_e(-\delta)] + n[T_i(\delta) - T_i(-\delta)] \end{gathered} \tag{3.17}$$

Since $\delta \ll l$, the differences $T_a(\delta) - T_a(-\delta)$ and $n(\delta) - n(-\delta)$ are equal to the jumps (3.12) in concentration and temperatures at the mirror with the accuracy of terms of order δ/l. With allowance for this we can rewrite (3.17) in the form

$$\begin{gathered} \frac{x_a}{l}(\Delta T_a - \delta T_a) = Q_a - \frac{5}{2} q T_a \\ T_a \Delta n + n \Delta T_a = n(\delta T_e + \delta T_i) + (T_e + T_i)\delta n \end{gathered} \tag{3.18}$$

Together with Eqs. (3.14), Eq. (3.18) forms an algebraic system of equations relating the jumps δn and δT_a with the total drops Δn and ΔT_a.

The solutions of this system, which are, in general, cumbersome, are considerably simplified if the dimensionsless parameter $\lambda k/l$, which figures in (3.18), is small or large compared with unity. For example, in the case when $\lambda k/l \gg 1$ the solutions have the form

$$\delta n = \Delta n, \quad \delta T_a = \Delta T_a \tag{3.19}$$

In this case the entire drop in density and temperatures occurs in the region of the

mirror. In the opposite limiting case of $\lambda k/l \ll 1$ the changes in n and T_a are distributed more uniformly along the mirror cell, while the jumps at the mirror are

$$\delta n = \frac{7}{9}\left[\Delta n + n\frac{\Delta T_e + \Delta T_i}{T_e + T_i}\right], \quad \delta T_e = \frac{kx_e}{nl}\left[\frac{\pi m_e}{2T_e}\right]^{1/2}\Delta T_e \tag{3.20}$$

$$\delta T_i = \frac{2}{9}\left[\frac{\Delta n}{n}(T_e + T_i) + \Delta T_i + \Delta T_e\right]$$

By substituting Eqs. (3.19) or (3.20) into Eqs. (3.14) we arrive at the desired expressions for the fluxes of matter and energy for the assigned drops Δn and ΔT_a between the centers of the mirror cells.

$$\lambda k/l \ll 1$$

$$q = -\frac{8}{9k}(2\pi m_i T_i)^{-1/2}[(T_e + T_i)\Delta n + n(\Delta T_e + \Delta T_i)]$$

$$Q_e = -x_e\frac{\Delta T_e}{l} \tag{3.21a}$$

$$Q_i = -\frac{20}{9k}\left[\frac{T_i}{2\pi m_i}\right]^{1/2}[(T_e + T_i)\Delta n + n(\Delta T_e + \Delta T_i)]$$

or

$$\lambda k/l \gg 1$$

$$q = -\frac{(2\pi m_i T_i)^{-1/2}}{k}\left[(T_e + T_i)\Delta n + \frac{1}{2}(\Delta T_e + \Delta T_i)\right]$$

$$Q_e = -\left[\frac{2T_e}{\pi m_e}\right]^{1/2}\frac{n}{k}\Delta T_e \tag{3.21b}$$

$$Q_i = -\frac{1}{k}\left[\frac{T_i}{2\pi m_i}\right]^{1/2}[(T_e + T_i)\Delta n + 3\Delta T_i + \Delta T_e]$$

The further procedure for the derivation of the equations describing the time and space distribution of the plasma parameters is analogous to that described in Section

2.1. We will confine ourselves to the consideration of one particular case, which is of practical interest, of the evolution of rather long plasmoids with $L \gg l(m_i/m_e)^{1/4}$, when the temperatures of the electrons and ions are able to become equal to each other and equalized along the magnetic field in the time of expansion:

$$T_e = T_i = T, \quad \frac{\partial T}{\partial s} = 0 \tag{3.22}$$

Under these conditions the dynamics of the plasma is described by a single equation for the concentration. Substituting q from (3.21) into (2.8) and keeping (3.22) in mind, we obtain the equation for n:

$$\frac{\partial n}{\partial t} = D\frac{\partial^2 n}{\partial z^2}, \quad D = \begin{cases} D_1 = \dfrac{8l}{9k}\left[\dfrac{2T}{\pi m_i}\right]^{1/2}, & l_m \ll \lambda \ll l/k \\ D_2 = \dfrac{l}{k}\left[\dfrac{2T}{\pi m_i}\right]^{1/2}, & l/k \ll \lambda \ll lk \end{cases} \tag{3.23}$$

The equation formulated describes the process of diffusional expansion of the plasma along the magnetic field. The inequalities pertaining to the coefficient of diffusion are obtained through a combination of conditions (1.10) and the inequalities $\lambda k/l \ll 1$ and $\lambda k/l \gg 1$ which were used in solving the system of equations (3.18).

By using Eq. (3.23) one can estimate the velocity of expansion u and the time of longitudinal confinement $\tau \approx L/u$, of the plasma, by a corrugated field, in the range of mean free paths (1.10)

$$u \sim v_{Ti}\frac{l}{Lk}, \quad \tau \sim \frac{L}{v_{Ti}}\frac{lK}{l}$$

that coincides with the estimate (1.11) obtained, approximately in Section 1.

At the limits of their applicability with respect to mean free path the equations obtained can be compared with the corresponding equations derived in Section 2.3 and in Section 3.1. The results presented here are intermediate between the purely kinetic and purely hydrodynamic models analyzed above, and along with these results they give a complete picture of the dynamics of plasma flow in a strongly corrugated ($k \gg l$) magnetic field.

3.3 The "Plateau" Regime of Plasma Motion in a Weakly Corrugated Magnetic Field

As was already discussed in Section 1, among the various regimes of plasma motion in a weakly corrugated magnetic field there is one of the intermediate type, which corresponds to the transition between the limiting cases of small-scale and large-scale corrugation studied in Section 2.4 and Section 3.1. It is realized under the condition that the transition time of trapped particles to untrapped ones is smaller than the bounce time of the trapped particles (see (1.5)), while at the same time $\lambda \gg l$. In the opposite case with $\lambda \ll l$ the flow becomes pure hydrodynamical and is described by the equations obtained in Section 3.1.

With fast exchange between trapped and the transiting particles the phase space distribution is close to a Maxwellian. The mechanism of transfer of momentum from the plasma to the magnetic field is quite analogous to Landau damping. The effect is well known in a "neoclassical" theory of transport phenomena in toroidal devices [17]. It is convenient to consider it quantitatively by means of the same approach used in Section 2.4, that of finding an average over one mirror cell of the friction force

between plasma and magnetic field. Based on paper [21], we present details of the calculation.

The frictional force (2.30) is determined by the correction to the Maxwellian distribution which can be found in a linear approximation with respect to a field modulation from the collisionless version of the kinetic equation (2.29). Integrating this equation over the trajectories of unperturbed motion $s = s_0 + v\cos\theta t$, we find

$$f_i = -F_{Mi}\frac{m_i uv}{T}\frac{\sin^2\theta}{\cos\theta}\frac{H(s) - H(s - vt\cos\theta)}{H(s - vt\cos\theta)}, \qquad (3.24)$$

where it is taken into account that the unperturbed distribution function is a "shifted" Maxwellian. Substituting (3.24) into (2.30) and integrating over θ in the limit $t \to \infty$ (such that the main contribution in integral (2.30) results from the values of θ close to $\pi/2$) we get the expression for frictional force.

$$F_{fr} = -\left[\frac{2}{\pi}\right]\frac{nu(T_i m_i)^{1/2}}{H^2 l}\int_0^l ds\,\frac{dH}{ds}\int_{-\infty}^{+\infty}\frac{H(s) - H(s - s')}{s'}ds' \qquad (3.25)$$

Making use of the periodic structure of the magnetic field the integration over an infinitive interval can be substituted by a sum. This sum is calculated in an explicit form, which is convenient for finding the values of F_{fr} under the various magnetic field profiles:

$$F_{fr} = -\frac{(2\pi T_i m_i)^{1/2} nu}{H^2 l^2}\int_0^l \frac{dH}{ds}ds\int_0^l [H(s) - H(s - s')]\,ctg\,\frac{\pi s'}{l}ds' \qquad (3.26)$$

The velocity of the slow plasma expansion can be found from the balance of forces which is quite similar to that used in Section 2.4. Under the conditions $T_e = T_i = T$, $\partial T/\partial z = 0$ all information about the plasma evolution is given by the

diffusive equation for the plasma density

$$\frac{\partial n}{\partial t} = \frac{\partial}{\partial z} D \frac{\partial n}{\partial z} \tag{3.27}$$

$$l \ll \lambda \ll l(k-1)^{-3/2} \ll L(k-1)^{1/2}$$

$$D = \left[\frac{2}{\pi}\right]^{3/2} \frac{T^{1/2} l}{m_i^{1/2}(k-1)^2}$$

The numerical coefficient in the expression for D corresponds to a sinusoidal profile (2.35). The set of inequalities provides the condition for the plateau regime and the smallness of the expansion velocity in comparison with the ion thermal velocity.

One of the possible applications of this theory was developed in [37] to explain the data obtained in Novosibirsk experiments with an alkali plasma. The experiments were carried out in the multiple mirror field with 11 mirror cells with two values of mirror ratios; $k = 1.83$ (moderate corrugation) and $k = 1.15$ (weak corrugation). As to results for $k = 1.83$ it will be discussed later in Section 5. Here it is reasonable to concentrate on the results related to the case of weakly modulated magnetic field.

In these experiments the density drop Δn in a steady state alkali plasma flow was measured while it passed through 11 mirror cells. The values of the density and the temperature were such that the regime of plasma flow was within the scope of the plateau regime. The last inequality in (3.27) $l/L' \ll (K-1)^2$ was not satisfied so the frictional force was comparatively small and could not produce a large decrease of the flow velocity in comparison with thermal velocity; correspondingly, $\Delta n/n \ll 1$. Since the plasma velocity was high ($u \simeq v_{Ti}$), the factor $\exp(-m_i u^2/2Ti)$ was added in (3.26) to take this into account.

For comparison of the experimental result with the theory the two-fluid gas dynamic equations with frictional force (3.26) was analyzed:

$$nu = \text{const}$$

$$m_i nu \frac{\partial u}{\partial z} = -\frac{\partial}{\partial z}(p_e + p_i) + F_{fr} \tag{3.27}$$

$$e\, n\, E = -\frac{\partial p_e}{\partial z}$$

Because of the high electron thermal conductivity, the flow of electrons in all of the regimes is isothermal, while the ion component has a very low thermal conductivity. Under these conditions, the work performed by the electric field on the ion motion can be given by

$$\frac{\partial}{\partial z}\left[\frac{m_i u^2}{2} + \frac{5}{2} T_i\right] = e\, E \tag{3.28}$$

Combining expressions (3.27) and (3.28) one gets the equation for the plasma density

$$\frac{\partial n}{\partial z}\left[T_i + \frac{3}{5}(T_e - m_i u^2)\right] = F_{fr}$$

Taking the frictional force as a perturbation one finds the density drop

$$\frac{\Delta n}{n} = 11 \frac{(T_i m_i)^{1/2} u (k-1)^2}{T_i + \frac{5}{3}(Te - m_i u^2)} \exp(-m_i u^2/2T_i) \tag{3.29}$$

The numerical coefficient corresponds to the field profile (2.35).

The value of $\Delta n/n$ depends on a number of parameters which can vary over wide ranges. Taking into account the possible experimental variations of the values of T_i, T_e, and u one can use (3.29) to estimate $\Delta n/n \simeq 0.3 - 0.5$, in good agreement with

the experimental data.

3.4 The Effect of Heavy Impurities on Multiple Mirror Confinement

The results presented above and in Section 2 cover practically all of the possible cases for hydrogen plasma flow in multiple mirror fields. New possible conditions of plasma flow appear if a small amount of a heavy impurities is added to the device. Inserting the impurities with $Z \gg 1$ allows, as will be shown below, considerable improvement of multiple mirror reactor characteristics.

At a temperature $T = 10$ keV the fusion power output in a pure DT-plasma is known to be approximately 30 times greater than the bremsstrahlung losses. By inserting the impurities with a charge $Z \gg 1$ the bremsstrahlung losses rise by a factor of $n_Z Z^2/n_H$, where n_Z and n_H are, respectively, the densities of impurities and of hydrogen isotopes (the density of impurities is assumed to satisfy the condition $n_Z Z \leq n_H$, for which the electrons have mainly a "hydrogen" origin). Then the ultimate permissible density of impurities is determined by the condition

$$n_Z Z^2/n_H \leq 30. \tag{3.30}$$

On the other hand, at densities $n_Z Z^2/n_H \geq 1$ the impurities can considerably increase the scattering frequency of hydrogen ions. It was suggested in [38] to use this circumstance to decrease the absorbtion length of CO_2-laser radiation in a plasma (the absorbtion length is inversely proportional to the scattering frequency of electrons on ions). It is evident that by inserting impurities one can reduce the absorption length by an order of magnitude without violation of the condition (3.30). It is obvious that, in the same way, one can appreciably reduce the length of a multiple mirror trap [39, 40].

Indeed, if $n_Z Z^2/n_H \geq 1$, the hydrogen ions scattering path decreases by a factor of $n_Z Z^2/n_H$ in comparison to the case of a pure hydrogen plasma. The scattering path reduction results in a slowing down of the plasma diffusion along the multiple mirror magnetic field. This allows a reduction in the installation length needed to provide the given confinement time.

In the case of $n_Z Z^2/n_H \geq 1$ the hydrogen ions mean-free path λ_{HH} with respect to the collisions between themselves is connected to their mean-free path λ_{HZ} with respect to the collisions with impurities and with impurity mean-free path λ_{ZZ} by the relationships: $\lambda_{ZZ} \sim \lambda_{HZ}/Z^2 \sim \lambda_{HH}\, n_H/n_Z Z^4$. For the quantitative illustration of the impurity effect on the expansion velocity, the case will be examined when the spacing l between two mirrors is smaller than the minimum scattering length, λ_{ZZ}. All species of particles are therefore in the small scale corrugation regime. The longitudinal diffusion coefficients of the various components according to (2.28) can be estimated by the following relations

$$D_e \sim v_{Te}\, \lambda_{HZ}/k^2, \qquad D_H \sim v_{TH}\, \lambda_{HZ}/k^2, \qquad D_Z \sim v_{TZ}\, \lambda_{ZZ}/k^2 \tag{3.31}$$

(the mirror ratio k is taken to be large, $k \gg 1$, and the width of the mirrors is assumed to be smaller than the distance l between them). Here, in an order of magnitude estimates, we neglect the difference between deuterium and tritium masses.

The estimates (3.31) show, that the electron diffusion is fast compare to the other particles. However, in the case when the plasma expands into a vacuum the electrons move together with the light ions due to the effect of a polarization electric field. As to the heavy ions, they can be regarded as immovable (due to their very small diffusion

coefficient) within the scale of the light component expansion time.

Based on the estimates (3.31), let us compare, numerically, the case of confinement of a pure DT-plasma with that of a plasma with a small heavy ion admixture. For the parameters $T \sim 10$ keV, $n \sim 3 \cdot 10^{17}$ cm^{-3}, and mirror ratio $k = 3$, with pure DT-plasma confinement, to obtain the Lawson time, $t_L \sim 3 \cdot 10^{-4}$ sec, the length L of the multiple mirror device, is of the order of 30 m. If 10% of impurities with $Z = 10$ are inserted, the length of the machine can be reduced to 10 m (to obtain this, one should note that for a given confinement time, the installation length is proportional to the square root of a diffusion coefficient). However, in this case the mean-free path λ_{ZZ} equals 0.6 cm, so it is rather hard to satisfy the condition $l < \lambda_{ZZ}$ with a reasonable installation diameter. Therefore we shall analyze the case of $\lambda_{ZZ} \ll l \ll \lambda_{HZ}$.

Over this range of parameters the impurity flow is purely hydrodynamic ($\lambda_{ZZ} \ll l$), while the light ion motion corresponds to the regime of a small-scale corrugation. The expansion velocity of a heavy component is defined by the balance of two forces: the accelerating force, which is due to the polarization electric field and the friction force against the magnetic field, which is connected with a longitudinal ion viscosity: $\eta_{HZ} u_Z / l^2 \sim eZn_Z E$ (this estimate holds for not too large mirror ratios, $k - 1 \sim 1$). Hence, taking into account that $\eta_{HZ} \sim \lambda_{ZZ} v_{TZ} Z M_Z n_Z$ and $E \sim T/eL$, one gets $u_Z \sim v_{TH} \sqrt{Z}\, l^2 / \lambda_{ZZ} L$. Comparing this with (3.31), we find the condition $l < Z^{3/4} \lambda_{ZZ}$ for the heavy component expansion to be slower than the light one. For the numerical example considered above this inequality gives $l \lesssim 5$ cm; this estimate is quite acceptable if an installation radius is smaller than 2 – 3 cm.

Since in the case of $l < Z^{3/4} \lambda_{ZZ}$, the heavy ions can be considered as immovable within the scale of a light component expansion time, the exact equations describing a light component flow can be obtained in the way analogous to that used in Sections 2.1–2.3. Thereby it is quite sufficient to take into account only the collisions of electrons and light ions with heavy ions (Lorentz plasma model). As was shown in Section 2.3, the temperatures of all species can be considered to be equal ($T_e = T_H = T_Z = T$) and constant ($\partial T / \partial x = 0$) along the plasma column which holds in many cases of practical interest. Under these assumptions the equations for deuterium and tritium densities have a form:

$$\frac{\partial n_{D,T}}{\partial t} = \frac{3T^{5/2}}{\sqrt{2\pi^3}\, m_{D,T}^{1/2}\, \Lambda e^4 Z^2 K^2} \frac{\partial}{\partial x} \left\{ \frac{1}{n_Z (n_D + n_T)} \left[(2n_{D,T} + n_{T,D}) \frac{\partial n_{D,T}}{\partial x} + n_{D,T} \frac{\partial n_{D,T}}{\partial x} \right] \right\}$$

where Λ is the Coulomb logarithm and $n_Z \equiv n_Z(x)$ is an initial distribution of impurities (the polarization electric field is excluded by means of a quasinetrality condition). These equations allow one to predict a time-space evolution of a DT-plasma with heavy impurities in a multiple mirror magnetic field. The practical use of these equations for impurity parameter optimization has several difficulties since the conditions of their applications can be easily violated under the parameter variation. To derive the equations which have no such disadvantages another approach was developed. It is based on a less accurate but a more convenient force balance equations for each group of particles (deuterium and tritium ions were considered as one group with $m_i = 2.5 m_H$). A brief description of this equation was published in [41] and a detailed one with the analysis of the results of optimization was given in [42]. Since this theory

was mostly developed in an application to the problem of reactor parameter optimization we will discuss it in the next section, devoted to different aspects of reactors.

4. MULTIPLE MIRROR REACTOR CONCEPTS

The general theoretical treatment can be used to quantitatively optimize the different types of multiple mirror fusion reactors. With this objective we will present a brief review of these studies. Two main types of multiple mirror reactor were studied: a pulsed reactor with dense plasma, first described in [43], heated by relativistic electron beams and confined in the radial direction by a magnetically insulated rigid wall (so-called "wall' confinement); and a steady-state reactor with magnetic confinement, first described in [27]. The procedure of optimization of axial confinement for the pure D-T pulsed reactor is described in Section 4.1. In the same Section the results of a quantitative analysis of the effect of heavy impurities is presented. The physics of the radial nonmagnetic confinement and the complete concept of the pulsed multiple mirror reactor with $\beta \gg 1$ are discussed in Section 4.2. Section 4.3 is devoted to a review of the optimization of steady-state multiple mirror reactor confinement. The stability, radial confinement, and complete concept are considered in Section 4.4.

4.1. The Optimization of the Axial Confinement of a Pulsed Reactor

Comparing (1.1) with (1.11) one can see that the corrugation of the magnetic field allows an improvement of pulsed reactor characteristics of approximately a factor of 10k. We now consider what a more accurate analysis, based on the equations presented in Section 3.3, gives. The case of pure D-T plasma was treated in [44]. The statement of the problem was very close to that described at the beginning of Section 1. At

$t = 0$ the initial space density distribution, initial temperature T_0, which was assumed to be constant along z, and the energy W_0 per unit of transverse plasma cross-section were fixed. A numerical integration of the equation (2.28) for $t > 0$ determined the time evolution of the space density distribution while the time evolution of the temperature was found by including the plasma cooling due to the bremsstrahlung radiation, the end losses, and the α particle heating. With this data the fusion energy output per unit of plasma cross-section was calculated during the plasma expansion along the multiple mirror field. Dividing this value by W_0 one finds the reactor Q.

One feature of the small scale corrugation regime (2.28), is that the peak value of the initial density distribution n_0 and the length of the installation L do not come into the expression for Q separately, but in the combination n_0L. This product can be expressed in terms of T_0 and W_0 so the value of Q can be analyzed as a function of only these two parameters. The study of the dependence $Q(T_0)$ with a given value of W_0 showed that a maximum value of this function is achieved with $T_0 = 4 - 5$ keV, which is, therefore, the optimal range of values from the point of view of axial confinement.

The energy supply W_0 required for the achievement of moderate values of Q ($Q \simeq 1$) to some extent exceeds the value obtained from estimate (1.11). This difference arises because plasma cooling is faster than particle loss from the system. It results from the higher energy losses through the electron channel if one assumes that each electron takes out energy of the order of $5T_e - 6T_e$. (This electron energy loss may be recovered.) The possibility of reducting the requirements of the reactor param-

eters by allowing the mirror ratio k to increase toward the ends of the system was analyzed in [44]. It allows a reduction of the value of W_0 by approximately 1.5.

Finding the optimal values of T_0 and W_0 for each value of Q one can calculate values of n_0L. It is obvious that by means of choosing higher values of density the length of the system can, in principle, be made shorter. The main limitation on n_0 in [44] is concerned with the limitation on the pressure which the containing walls can support. To illustrate the results of an optimization we show the dependence of the length of the reactor for the achievement of given values of Q under the different values of n_0 and correspondingly, pressure p_0.

TABLE 1

Pulsed multiple mirror reactor axial confinement including α-particles heating ($k = 2$)

	$Q = 0.4$ ($W_0 = 2.5$ MJ/cm^2)	$Q = 1$ ($W_0 = 5$ MJ/cm^2)	$Q = 4$ ($W_0 = 10$ MJ/cm^2)
$n = 8 \cdot 10^{16}$ cm^{-3} $p_0 = 1000$ bar	170 m	340 m	700 m
$n = 2 \cdot 10^{17}$ cm^{-3} $p_0 = 3000$ bar	60 m	120 m	230 m

The possibility of further improvement of the reactor characteristics by inserting a small amount of heavy impurities into the plasmoid was studied in [41,42]. Before description of the accurate optimization theory we will estimate the value of expected effect. Let us define W_Z as the energy input needed for the reactor with impurities and W as the energy without impurities, which produce the same values of Q. We

introduce then the energy lifetime $\frac{1}{\tau} = \frac{1}{\tau_{\|}} + \frac{1}{\tau_r}$, where $\tau_{\|}$ is the time of the axial confinement; $\tau_r \sim W_Z/P_r(1+\mu)$ is the time of Bremsstrahlung losses, where the factor $\mu = n_Z Z^2/n$ takes into account the presence of the impurities. Taking into consideration that the fusion power $P_f \simeq n^2 L f(T) \simeq 30 P_r$ and $W \simeq nTL$, one finds

$$\frac{1}{Q} = \frac{W_Z}{P}\left[\frac{1}{\tau_{\|}} + \frac{1}{\tau_r}\right] \simeq \frac{1}{W_Z^2 F(T)(1+\mu)} + \frac{1+\mu}{30}$$

where the function $F(T) \sim f(T)/T^{1/2}$ should be optimized with respect to temperature. Noting further, that if $\mu = 0$ we have

$$\frac{1}{Q} = \frac{1}{W^2 F(T)} + \frac{1}{30},$$

we can substitute $F(T)$ with W^2. If one neglects the difference between optimal temperatures for the plasma with and without impurities (the numerical factor 30 changes a little with the temperature) then the relation W_Z/W can be written as follows:

$$\frac{1}{Q} = \frac{W^2}{W_Z^2(1+\mu)}\left[\frac{1}{Q} - \frac{1}{30}\right] + \frac{1+\mu}{30}.$$

Maximizing W_Z/W the maximum improvement from impurities is achieved for $1+\mu = 15/Q$ and it equals

$$\frac{W_Z}{W} = \sqrt{Q/7.5}$$

If one considers another statement of the problem and calculates the increase in Q that can be obtained when W is fixed, the result is the same,

$$Q_Z/Q \simeq \sqrt{7.5/Q}.$$

This consideration shows the main characteristic features of the effect of the impurities, which plays a small role for values of $Q \geq 5$. On the other hand for increasing values of Q α-particle heating becomes of more and more importance in the energy balance. The estimate obtained shows that for $Q \simeq 2-3$, the impurities allow a reduction of W by about a factor of 2. Larger effects can be achieved by means of an inhomogeneous initial impurity density distribution, with impurities mostly located within the maximum of the plasma density gradient.

The search for an optimal form of the impurity density distribution, and the value of the temperature and the other plasma parameters, was carried out by means of a numerical solution of the equations which describe the self-consistent motion of the plasma and heavy impurities. The problem was analyzed in the same way as described above for pure D–T plasma. Given, at $t = 0$, the initial plasma and impurity density distributions find the slow (in comparison with thermal velocity) diffusive flow of each of the components, the pressure gradient, the electric field, the joint frictional forces, and the friction of the magnetic field. Macroscopic equations for the velocities u_H, u_Z of the components, which follow from the balance of these forces, have a form

$$-n_H u_H m_H v_{TH}\left[\frac{\alpha}{\lambda_{HZ}} + \frac{\beta}{\lambda_{HH}}\right] - \gamma\frac{n_H M_H v_{TH}}{\lambda_{HZ}}(u_H - u_Z) + e n_H E - \frac{\partial p_H}{\partial Z} = 0$$

$$-\gamma\frac{n_H m_H v_{TH}}{\lambda_{HZ}}(u_Z - u_H) - \frac{n_Z u_Z m_Z v_{TH}}{l} + \frac{1}{(l/\lambda_{ZZ} + \lambda_{ZZ}/l)} + eZn_Z E - \frac{\partial p_Z}{\partial Z} = 0$$

Here p_H and p_Z are, respectively, the pressure of the plasma and of the impurities. The factors α, β, γ, δ, η are the numerical coefficients which values depend on the geometry of the magnetic field and, correspondly, are functions of the mirror ratio.

The calculations, using this equation, showed that the optimal values of Z are in the range $Z \leq 10$. For small Q and optimal parameters the value of Q_Z increase 3 – 4 times in comparison with the case of a pure hydrogen plasma. Correspondingly the energy decreases by the same factor if Q is fixed. The comparison of the cases of homogeneous and inhomogeneous initial impurity density distributions shows that by the appropriate choice of the profile the effect of impurities can be increased by approximately 2 times. Similar effects were found for steady-state reactors [45], and will be discussed, briefly in Section 4.3.

In considering the thermonuclear aspects of multiple mirror axial confinement one should keep in mind that only the ions with $\lambda/k \ll L$ are effectively confined in these systems. We suppose that this condition is fulfilled for most of the particles, but this can be violated for high energy ions with $\lambda(\varepsilon)/k \geq L$. Since it is the high energy particles that give the main contribution to D–T fusion power output, it is essential to clarify how large is the difference between the actual distribution function and the Maxwellian one at high energies. This problem was resolved in [46]. This difference was shown to be insignificant at large mirror ratios ($k \geq 3$), but at small k it is possible to have some decrease of the neutron yield. In the same paper it was found that the addition of some impurities does not lead to a noticeable variation of the Maxwellian distribution provided $n_Z Z^2/n < (Lk/\lambda)^{1/2}$. At high concentrations of impurities there is a substantial deviation of the distribution function from a Maxwellian.

4.2. The Complete Pulsed Reactor Concept

The procedure of axial confinement optimization described above allows us to minimize the value of the initial energy input per unit of plasma cross-section. The full amount of energy that is needed for the achievement of the given value of Q is determined by the transverse size of the system. The axial optimization of a pulsed reactor shows that for reduction of the length of the reactor to 100 m it is necessary to use the plasma with high density $n \geq 3.10^{17}\,\mathrm{cm}^{-3}$. At a temperature $T_0 = 5$ KeV magnetic containment requires the use of magnetic fields in the megagauss range which is not practical. For this reason, for a pulsed multiple mirror reactor, "wall" confinement is employed. The magnetic field is then required only to reduce the transverse heat conduction, and radial equilibrium is provided by the rigid walls. Besides the obvious features, concerned with the contact between plasma and wall, substantial differences appear in plasma behavior as a whole. Most important of these are convective plasma and magnetic field motions, which are practically absent in plasma with $\beta < 1$, but become dominant in the case $\beta \gg 1$.

A number of papers have been devoted to theoretical study of these questions. In most of them a pure transverse problem is analyzed, in which the magnetic field and plasma parameters are considered to change only along the radius and to be homogeneous along the z-axis which coincides with the direction of the magnetic field. Since the plasma is considered to be heated by means of a relativistic electron beam (REB), the problem of initial conditions was studied which correspond to the radial cold plasma density distribution which is homogeneous in the direction of the magnetic

field. The heating pulse and the plasma cooling processes are described with one-fluid MHD equations. The analysis of the cooling rate allows one to find the scaling of the transverse confinement time $\tau_\perp(R)$, then the optimal value of the plasma radius can be found from the condition $\tau_\perp(R) = \tau_\parallel(L)$.

The analytical study of the plasma cooling process is very complicated because of the strongly inhomogeneous profiles $n(r)$, $T(r)$, $H(r)$ which are created due to the passage of an REB through the plasma bunch. The first numerical calculations [25] showed that the plasma cooling rate is approximately 10 times faster that follows from the simple estimate

$$\tau_\chi = R^2/\chi_\perp \tag{4.1}$$

where $\chi_\perp$ is the coefficient of thermal conductivity.

There is now a clear understanding of the physical mechanisms which are responsible for the resulting thermal conductivity becoming much greater than the classical value (4.1) (see review [27]). The main feature of nonmagnetic confinement is that the plasma pressure remains almost uniform in the radial direction during cooling: nT = const. Hence, the temperature drop near the wall causes a corresponding rise in the density which is provided by plasma convective flow from the center to the wall. Although the velocity of this plasma radial expansion is much slower than the thermal velocity, it can (as shown in [27]) be considerably higher than $\chi_\perp/R$, the velocity of propagation of the cooling wave. Thus the convective plasma flow results in a cooling time for the plasma which is much shorter than the estimate of (4.1). In the case, for example, of nonconducting walls the cooling time can reach the value of the Bohm

time, despite the classical values of the transport coefficients.

These results are mostly related to the case of the uniform initial density distribution of the cold plasma. The numerical calculations [26,41] showed that by means of the choice of nonuniform initial density distribution the confinement time can be increased by an order of magnitude as compared to the uniform case. If, for example, the plasma occupies the central part of a tube before the beam is switched on, it expands during heating and compresses the magnetic field in the gap until its pressure becomes locally equal to the plasma pressure. As a result, the hot plasma is isolated from the walls by the magnetic field. Since the diffusion of a magnetic field is $(m_i/m_e)^{1/2}$ times slower than temperature conductivity the cooling time increases. The efficiency of this method is limited by the finite time of the magnetic field diffusion into the chamber walls. This effect decreases the improvement of a nonuniform initial distribution with values of $\beta \simeq 100$ and it makes moderate values of $\beta \simeq 5 - 10$ more optimal. The final result of the computer study of the problem can be approximated by means of the expression for the transverse confinement time $\tau_\perp = 7.2 \cdot 10^{-2} \tau_\chi/\beta^{1/2}$ [41], where τ_χ is given by (4.1). From this calculation achievement of $Q = 1$ with $H = 100$ kG required a plasma radius not less than 4 – 5 cm.

The effect of the microinstabilities on the confinement time can be estimated, as usual, by introducing Bohm thermal conductivity $\chi_{\perp B} = (1/16)(cT/eH)$. It is interesting to note that, in contrast to the case of the classical transport coefficient, with Bohm scaling the rough estimate and the exact numerical calculations of the transport equations give approximately the same result. This is caused by the difference in the tem-

perature dependences of the Bohm and the classical coefficients.

Radiative effects during the cooling of high-β plasma were examined in a number of papers (see review [27]). We will not discuss them here since, in the parameter range close to the optimal reactor ones, they play no role. The additional impurity flux caused by contact between the plasma and the metallic walls can lead, in principle, to a large increase of the radiative losses. Consideration of the problem showed that the diffusion of heavy impurities into a dense plasma is substantially suppressed due to the convective plasma flux and the ion thermal force [47].

Apart from the microinstabilities that might result in an increase of the radial transport, flute-type MHD perturbations can be very dangerous for axisymmetric multiple mirror systems. They certainly would appear in the case of the magnetically confined plasma ($\beta < 1$) because of the considerable pressure drop along the radius. However, this instability is absent in the case when the plasma pressure is constant in the transverse direction (pure wall confinement). In a real situation of finite β there is an intermediate case; plasma pressure varies along the radius, but its variation does not exceed p/β. The study of the MHD stability of a $\beta > 1$ multiple mirror system carried out in [48] showed that variation of p along the radius equals, in order of magnitude, to just the value p/β. It means that the question of stability of the system depends on what concrete profile $p(r)$ is realized. Stable profiles of $p(r)$ certainly exist and one of them seems to be established automatically.

The effects of ion-ion viscosity have substantial influence on the dynamics of the flute instability in corrugated magnetic fields with $\beta \gg 1$. They result in the reduction of the growth rate by a factor $\beta^{1/2}$ [48]. If the inequality $\beta > N^2/\Lambda$ is satisfied then it

was found that the time for the development of the instability becomes greater than the axial confinement time. These arguments show that in wall confined systems the flute instability is not as dangerous as in traditional systems with $\beta < 1$.

In summarizing the optimization of the axial and radial confinement we will describe the parameters of a multiple mirror pulsed reactor with $Q = 1$ [49]. The full length of the reactor is equal to 60 m, radius of the chamber is 4 cm, magnetic field strength is 75 KG, and the mirror ratio equals 2. The maximum plasma density is $6 \cdot 10^{17}$ cm^{-3}, temperature is 5 keV, and the total energy is 120 MJ. A suggested method for plasma heating is by means of an REB with the use of a "two-stage" scheme. The main feature of this scheme is that the central part of the reactor is occupied by a smaller density plasma $n \simeq 10^{15}$ cm^{-3}, where the beam effectively transfers its energy by a collective interaction. This energy is, rapidly transported by the electron heat conductivity to the adjacent areas with the high density plasma which makes the main contribution to the fusion power output. For the parameters given above the heavy impurity improvement has been taken into account.

The operation of the reactor as practical energy source requires another optimization, which includes economic variables, which have not been considered above. A reactor has to operate with higher values of Q and there are more rigid restrictions on the maximum pressure and density of the plasma. These requirements result in a substantial increase of both the reactor size and its total energy. For example, including the reduction of the maximum plasma pressure below 500 atmospheres leads to the reactor length $L = 1000$ m.

4.3. Optimization of the Axial Confinement of a Steady-State Reactor

A steady-state concept for a multiple mirror reactor has the basic advantages over a pulsed concept that is shared by all reactor configurations. It also differs from the pulsed concept in a number of important respects, that can be either advantageous or disadvantageous. Because the average power must be held to reasonable levels, the density is much lower in a steady-state reactor than in a pulsed reactor. This requires longer confinement times to achieve a given reactor Q, requiring more attention to optimization of the magnetic field configuration in order to keep the reactor of reasonable length. The lower density opens the possibility of full magnetic confinement, with $\beta < 1$, which is reasonably well understood. However, since the axisymmetric field is not MHD stable, quadrupole fields are required to obtain stability, which can introduce new problems, both of a fundamental and practical nature. In this subsection we consider the results of the reactor studies considering only axial confinement issues. In the following subsection the MHD stability and radial transport issues will be considered.

As we have seen, when $l_m \ll \lambda \ll kl$ then there is a minimum local diffusion rate given by

$$D_{\min} = \frac{8}{9k}\left[\frac{2T}{\pi m_i}\right]^{1/2}$$

The steady-state operation of a multiple mirror reactor was studied [39] using a local diffusion coefficient slightly differing from this value [11]. The reactor model consists of a solenoid with multiple mirrors added to both ends. The central-solenoid length was assumed to be half of the device length and the multiple-mirror cells were

assumed to have equal cell lengths. Assuming an upper limit of 20 T for the superconducting solenoid coils, peak mirror fields of 30 T, and reasonable values of conversion efficiency from plasma loss energy and thermal neutron energy to electricity, then for $P_{\text{net}} = P_{\text{recirculating}}$ ($Q \equiv P_{\text{fusion}}/P_{\text{recirculating}} \simeq 2$) the reactor parameters were found to be: $L = 400$ m, $T = 4.5$ keV, and the central-cell density, $n_1 = 8 \times 10^{22}$ m^{-3} for $\beta = 0.8$. The system had 20 cells, each 5 m long, at each end. They also found that the breakeven reactor, $P_{\text{net}} = 0$ ($Q \simeq 1$) is 140 m long, and the ignited reactor, $P_{\text{recirculating}} = 0$, is 1100 m long. Since the density decreases towards the end of the machine and $\lambda \sim T^2/n$, the assumption of constant cell length leads to a device which does not operate in the ideal multiple-mirror regime near the ends, resulting in larger axial loss. Thus, the reactor length found in [39] is somewhat shorter than it would be if the axial loss were accurately computed.

Realizing this problem, a device with variable cell lengths was considered [45]. The cell lengths increase towards the end of the device to keep the plasma in the ideal multiple-mirror regime throughout the machine. In addition, it was assumed that the re-circulating power is provided by means of fast-neutral D-beam injectors. The fusion reactions between the fast beam particles and the background plasma increase the total fusion power over the studies of Logan et al., resulting in a shorter reactor. Both studies also assumed that the only loss processes are bremsstrahlung and axial loss; the entire alpha particle power is deposited in the plasma, and $T_e = T_i = T$. For the same central mirror ratio, magnetic field and β as in the previous study, for $Q \simeq 2$ they found $L = 340$ m. The second study did not include a long central solenoid, but rather a central cell which operates in the same mean-free-path regime as the other cells,

which results in a reactor length about 13% longer than a reactor with optimum central-cell length.

Another mode of operation was also studied called the wetwood-burner mode (pure-T background plasma) with depressed ion temperature [51]. In the wetwood-burner mode, the fusion power is produced by reactions between plasma T and beam D ions. In this case, Q increases with T_e while Q is almost independent of T_i because the background ion temperature is low compared to the beam energy, E_b ($T_i \ll E_b$). Since the axial power loss scales as $T_i^{7/2}$, depression of the ion temperature results in a shorter MMR for a given Q. By adjusting the reactor parameters so that most of the beam and alpha particle power is deposited in the electrons, one can make the ion temperature lower than the electron temperature. It was found that the depression of the ion temperature can be achieved by using high-energy neutral-beam injectors ($E_b \sim 170$ keV) in MMRs with only a few (5 to 15) cells to make $\tau_{mm} \cong \tau_{eq}$, ($\tau_{eq}$, is the electron-ion equilibration time). For a central-cell field of 9.3 T and a peak mirror field of 16 T, the reactor parameters were found to be: $T_e = 5.6$ keV, $T_i = 3.1$ keV, $E_b = 170$ keV, $n_1 = 5.8 \times 10^{21}$ m^{-3}, and $L = 230$ m for $\beta = 0.8$. The resulting value of $Q \approx 1.1$ was probably too low to be viable, even considering a blanked multiplication of approximately 1.5.

These studies [39, 45, 51] ignored the pressure of the alpha particles and assumed that the entire alpha particle power is deposited in the plasma. However, the alpha particles which are born in the loss cone carry almost all their energy out of the system. Furthermore, some of the confined alpha particles scatter into the loss cone while they are slowing down. Therefore, only about 80% of the alpha particle power (for $R \sim 3$

and $T_e \sim 5$ keV) will be deposited in the plasma, which results in a longer MMR.

Based on the reactor studies [45, 51], a cost analysis study of a MMR has also been performed [52]. Minimization of the unit direct capital cost ($\$/kW(e)$ output) was chosen as the optimization goal. The economic trade-offs among reactor length, magnetic field strength, mirror ratio, recirculating power fraction (or Q), wall loading and other related parameters were studied. It was found that the reactor cost versus Q shows a broad minimum in the range $Q \approx 5$ to 20; a MMR operating in the wetwood-burner mode, even though short, was not found to be economical, although optimistic unit costs were assigned to the recirculating power systems. The study also showed that, because of the B^2L = const scaling of MMR, the economics of the system favours high magnetic fields. In addition, the optimum mirror ratio and number of cells (and, therefore, the reactor cost) were found to be sensitive to the Joule losses in the mirror-quadrupole assemblies needed for average-minimum-B stabilization. The effects of the wall loading on reactor cost were also studied. Because of the high power density in a MMR, the first wall is located far from the plasma and the first-wall radius is basically determined by the desired wall loading. The study indicated that the optimum wall loading (minimum direct plus indirect cost of replacing the blanket) is about 1 to 2 MW m^{-2}.

The most complete steady-state reactor model took these various effects into account,and, although not explicitly considering cost optimization, used the results of that study to consider high central cell magnetic fields, and a relatively small total number of mirror cells [53]. Because of the small number of cells and the not-too-large value of k in the central cells a local diffusion model underestimates the density.

A cell-by-cell analysis, which we have already described in Section 3.2, can be used to obtain more accurate results. This was done using a somewhat different, but mainly equivalent, theoretical treatment [36].

The basic assumption for a steady-state MMR which consists of a central solenoid with length l_{c1} and multiple mirrors at both ends are as follows. The background plasma (the warm component) consists of deuterium ions with density $f_D n_i$ and tritium ions with density $(1 - f_D)n_i$, where f_D is the fraction of the D ion density of the total background ion density. The recirculating power, P_b, is supplied by means of fast-neutral D-beam injectors. The beam particles, slowing down in the plasma, form a hot component with density n_h and deposit part of their energy in the plasma (with $a_{eh}P_b$ going to electrons and $a_{ih}P_b$ going to ions). The remaining beam power, $a_{sh}P_b$, is lost because of the scattering of the beam particles into the loss cone. Fusion power is produced by reactions between hot D and warm T ions (P_{fh}) and warm D and T ions (P_{fw}). For other means of heating (e.g. ICRH), one can set $n_h = P_{fh} = 0$. Alpha particles, produced by fusion reactions, deposit some fraction of their power, P_α, into the plasma (with $a_{e\alpha}P_\alpha$ going to electrons and $a_{i\alpha}P_\alpha$ going to ions). The remaining power, carried by either the particles which are born in the loss cone or those that scatter into the loss cone, is lost ($a_{s\alpha}P_\alpha$). Particle loss and bremsstrahlung are the only loss processes; synchrotron radiation (unimportant in these low-T, high-n devices) and radial diffusion are ignored. Radial loss can be important in high-Q MMR and will probably determine the highest β at which a reactor can operate [54]. A comparison of the radial confinement time with the axial confinement time is given in the next subsection. As in the pulsed reactor the elimination of axial

heat flow to end walls requires insulating sheaths in an expanding plasma at the device ends, and the electron and ion temperatures are assumed constant throughout the device.

Using these assumptions, either in a diffusion model or a cell-by-cell matching model for the axial loss, an equation connecting all of the reactor parameters can be found in the form

$$p_1 L = f(Q, k_1, \frac{l_{c1}}{L}, \frac{\lambda_{\text{eff}}}{l}, 2N+1, T)$$

where p_1 is the central cell pressure k_1 is the mirror ratio of the central cell including pressure effects, l_{c1} is the length of the central cell, $2N+1$ is the total number of cells, and T is the temperature, assumed constant and equal for ions and electrons. For this calculation $f_D = .5$ and $n_h \simeq 0$. The quantity $\lambda_{\text{eff}}/l \simeq \lambda/kl$ is the ratio of trapping mean free path to cell length, which it is necessary to take into account because operation is in the transition region $\lambda_{\text{eff}}/l \sim 1$, where the formulas for large scale corrugation must be corrected. The results of an approximate correction given in [11] are used for the calculation. The magnitudes of the mirror field and β are taken to be constant in all cells, so that the mirror ratio k increases as the density decreases, and is therefore a variable in the optimization process. The optimization procedure is to minimize f to obtain a minimum of $p_1 L$ for a given Q, with k_1 taken as fixed. A simple optimization of T, as a function of $2N+1$ is then performed, with λ_{eff}/l is a parameter. The results of this study for a given Q are shown in Fig. 5. We see that good results are obtained with λ_{eff}/l in the range 0.2–0.25. As expected, the operation improves with increasing number of cells (the envelope of the λ_{eff}/l_c curves), with a reasonable

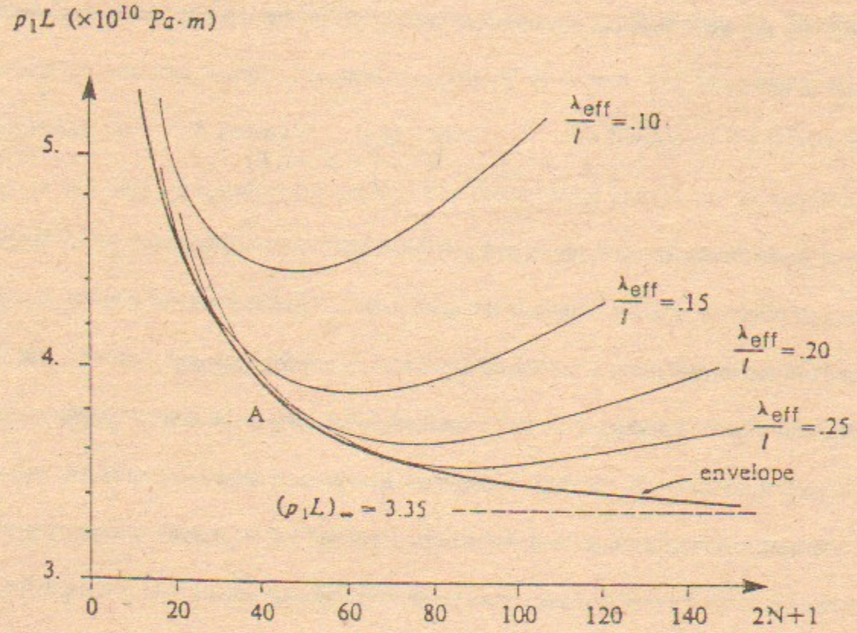

Figure 5. Optimum p_1L versus the number of cells $2N + 1$ for different values of λ_{eff}/l for $Q = 2$ and $k_1 = 3.36$.

operating condition with 20 cells on each end ($2N+1 = 41$), which was then held fixed for a study of other Q values. The economic optimum might well occur with fewer cells, e.g. ten cells on either end, with a 10 percent longer length. The complete set of reactor parameters for a range of Q-values is shown in Table 3.

TABLE 3

Parameters of a 41-cell MMR with $k_1 = 3.36$, and $\lambda_{eff}/l_c = 0.2$ ($\lambda/l_c = 1.4$)

Q	1	5	Ignition
T (keV)	4.6	6.0	7.4
l_{c1}/L	0.46	0.50	0.53
p_1L ($\times 10^{10}$ Pa·m)	2.5	6.3	12.5
B_1^2L ($\times 10^5 T^2 \cdot m$)[a]	0.8	2.0	3.9
L (m)[b]	312	773	1534
n_1 ($\times 10^{22}$ m^{-3})[b]	5.5	4.2	3.4

[a] $\beta = 0.8(R_v = 1.75)$.

[b] $\beta = 0.8(R_v = 1.75)$ and $B_1 = 16T$.

The results of this study included some conservative features that overestimated the energy flux and therefore predicted a larger p_1L than actually required. Recent unpublished work [55] indicates that considerable reduction in both length and magnetic field may be possible.

4.4. Steady-State Multiple Mirror Reactor

In common with tokamaks and tandem mirrors, multiple mirrors are at best ave-min-B devices. A magnetic configuration consisting of magnetic mirrors and linked quadrupole fields produces an ave-min-B well in a region near the axis [56]. As an example, choosing $l_m/l_c = 0.1$, and assuming a realizable form for the quadrupole field, the last stable radius at the midplane, r_w, is found to have a broad maximum of $r_w/R \approx 15\%$, where R is the mirror coil radius. These values are consistent with typical parameters of a steady-state reactor calculation for which $r_w = 3$ cm, $R \approx 50$ cm, and $l_c \approx 5$ m. One limitation of ave-min-B stabilization is the onset of localized (ballooning) modes with finite β. Calculations indicate, that substantial β's are possible in realistic reactor configurations [57, 58].

The fan shaped flux surfaces that are created by ave-min-B coils have certain undesirable features. The enhanced radial diffusion in the fans can add to the overall losses [59]. The asymmetry breaks the p_θ invariant that would otherwise prevent radial diffusion arising from nonadiabaticity. In addition, the quadrupoles increase the Joule heating in non-superconducting coils by about a factor of five and increase the complexity of coil design and construction [52].

The theoretical studies of the ave-min-B low β magnetic field structures explored the relationship between the well radius and flux surface ellipticities for various ratios l_m/l and mirror ratios. An idealized coil configuration was considered consisting of local mirrors and two sets of quadrupole bars, one carrying weak currents extending the full cell length l (the "weak quadrupoles") and quadrupole bars with strong

currents extending over the mirror scale length, with a mirror radius R (the "strong quadrupoles"). The well radius was optimized with respect to weak and strong quadrupole currents and strong quadrupole length. The results of the optimization are summarized in Fig. 6. In Fig. 6a the well radius at the center of the cell r_w is given, and in Fig. 6b the corresponding well radius in the mirror throat r_{min} is shown. Fortuitously, both large mirror ratios and small values of R/L, which are required for efficient longitudinal confinement, are more effective in producing large midplane wells. On the other hand, large mirror ratios also lead to large ellipticities, such that r_{min}/R decreases as the mirror ratio increases, leading to enhanced radial loss.

Although ave-min-B fields are subject to ballooning modes, which can limit the β of tandem mirrors, multiple mirrors do not appear to have such a limitation. The reason for this is that the unfavorable curvature is concentrated in a small region near the mirror throat, with a short connection length to the favorable curvature regions that extend over most of the cell. An approximate stability criterion can be written [57]

$$\beta_c \leq 8\pi^2 \gamma r_p R_c / l_m^2 ,$$

where γ is the ratio of average good curvature to the maximum destabilizing curvature R_c, r_p is the plasma radius, and l_m is the connection length. With the scalings for the multiple mirror, $\gamma \sim 0.1\, l_m/l_c$ and $R_c \sim l_c l_m / r_p$, the critical beta is predicted to be $\beta_c \leq 8$. These calculations were performed for practical geometries used in experiments, indicating stability at all $\beta \leq 1$ [57]. this work was extended to a general study of resistive ballooning which was more relevant to the experimental studies. The results were similar, except that resistive effects allow residual slow-growing modes

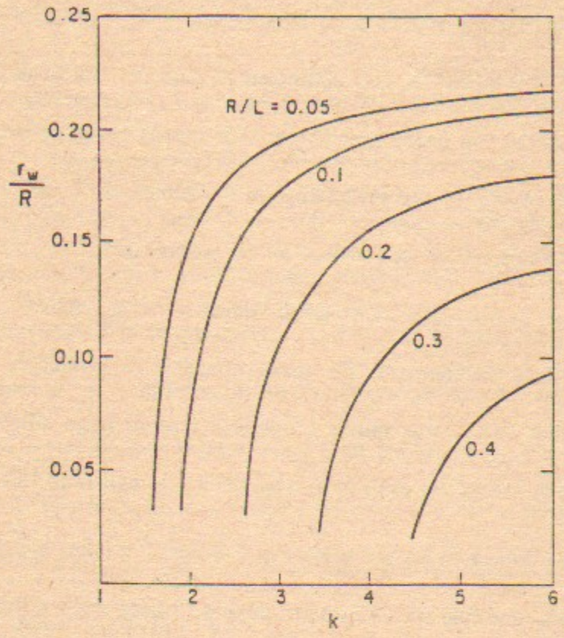

Figure 6a. Optimized well radius normalized to mirror radius versus mirror ratio.

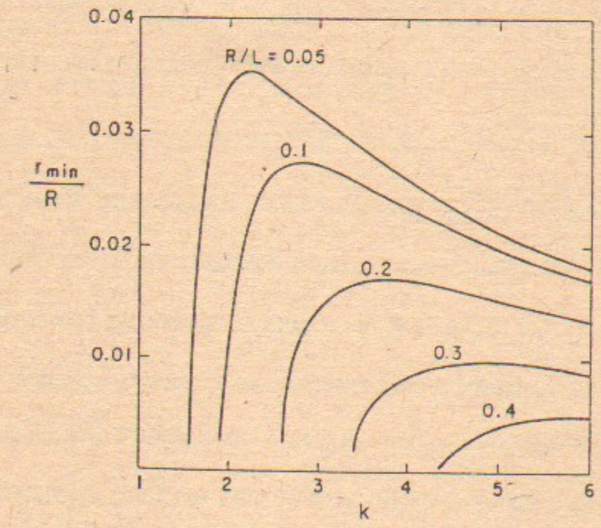

Figure 6b. The minimum well dimension in the mirror throat.

[58]. The resistive effects become unimportant under reactor conditions. The experimental results and comparison with the theory are given in Section 5.

Particularly for devices with β near unity, the radial diffusion time can become comparable to the axial diffusion time. In this case a more complete theory, including both radial and axial diffusion, is required. We have already given a simple estimate of the combined effect, for pulsed systems, in Section 4.2. For steady-state systems, in which the plasma is far from any radial wall, the actual process of combined radial and axial loss is that the central density diffuses radially toward the plasma edge, where the density is lower. At the lower density the axial diffusion is enhanced, so that all flux is eventually lost axially.

An analytic investigation of this combined phenomenon was made, showing that with proper definitions the overall confinement time could still be cast into the form

$$\frac{1}{\tau} = \frac{1}{\tau_z} + \frac{1}{\tau_r}$$

as used in Section 4.2 [54]. The theory shows that as $\beta \to 1$, the radial profiles are essentially flat with sharp gradients near the plasma edge. The results of the theory can be characterized in terms of a single parameter $\alpha \sim (\tau_z/\tau_r)^{1/2}$, and show that one can trust, quantitatively, a heuristic evaluation of the axial and radial loss using an effective mirror ratio $\bar{k}$ and an average magnetic field $\bar{B}$ given, even for values of β close to unity, by

$$\bar{k} = k_v \left[\frac{1 - \beta/k_v^2}{1 - \beta}\right]^{1/2}$$

and

$$\bar{B} = B_v(1 - \beta)^{1/2}$$

where k_v and B_v are the vacuum values of k and B, respectively. Radial losses are unimportant (e.g., less than 10% decrease in confinement time) for $\alpha \lesssim 0.5$. It was shown qualitatively that some improvement in overall confinement can be made by increasing the β of a system beyond the $\beta = 0.8$ value usually used in the calculations. However, for the usual parameters of steady-state reactors radial losses play a substantial role and cannot be neglected. Such designs should be optimized with the inclusion of the effect of radial losses.

5. EXPERIMENTAL EVIDENCE OF MULTIPLE MIRROR CONFINEMENT

Since the mean free path of the charged particles in plasma scales as $\lambda \propto T^2/n$, the predictions of the multiple mirror theory can be easily checked in a laboratory by using a wide range of temperatures and densities which correspond to the range of parameters for which $\lambda \sim l$. The steady state alkali plasma, obtained in Q-machines, is a very convenient medium for carrying out such experiments. Shortly after the first suggestions on multiple mirror confinement were published, these experiments were performed in Novosibirsk and Berkeley.

The first Berkeley installation had a length about 150 cm, the diameter was 6 cm, the number of mirror cells N could be varied from 1 to 5 and the mirror ratio could be varied from 1 to 4. The main part of experiments was carried out with $N = 5$, $k = 3.7$, and the mirror cell length $l = 28$ cm. The plasma, created by the ionizer near the one end of the device, was absorbed, after passing through the corrugated field, by a collector placed at the other end of the system. The length of the plasma column could be varied by moving the collector in the axial direction. The number of cells in the system could be changed either by moving the collector or by switching coils on or off. The plasma density was determined by Langmuir probes which measured the density distribution in the axial and radial directions.

The first results of the Berkeley experiments were published in [60] practically at the same time as paper [61] appeared giving results of experiments carried out at Novosibirsk. More detailed results of the Berkeley experiments were given later in

[27]. The experiments were performed over a wide range of densities 10^{-9} cm^{-3} $\leq n \leq 10^{11}$ cm, that made it possible to observe the behavior from the free Knudsen plasma flow at small densities to strongly collisional MHD flow at high values of density. In the first Berkeley experiments a comparatively small number of cells was used and there were no reliable information about radial losses. In addition, the ion temperature which is needed for the mean free path determination, was estimated from known alkali plasma properties. Despite these limitations, the results of the measurements of the effective plasma confinement time confirmed the theoretical predictions of the quadratic dependence on the number of cells and demonstrated, as well, the theoretical prediction of the dependence on the average mirror ratio.

An example of the experimental results is given in Fig. 7, which shows the probe current ($\propto$ density) in the first cell next to the source as a function of collector position in the (a) low, (b) intermediate, and (c) high density regimes. For the intermediate density case, the density at the source is seen to increase in a stepwise fashion as the collector passes each mirror throat, adding another cell to the system. (The first density jump corresponding to the collector passing the second mirror is a result of partial filling of velocity space due to ion trapping when the first cell is created, and is not a multiple-mirror effect.) The increases of the measured first cell density are smaller with the collector moving into cells 4 and 5, due to increasing radial loss. However, this can be taken account in the measurement of the longitudinal confinement time, by using the flux to the collector in the calculation. When this was done, the $\tau_{mm} \propto N^2$ scaling was obtained over all cells for the intermediate density case. The low density ($\lambda - L$) case and the high density ($\lambda \ll l$) case are characteristic of Knudsen flow and

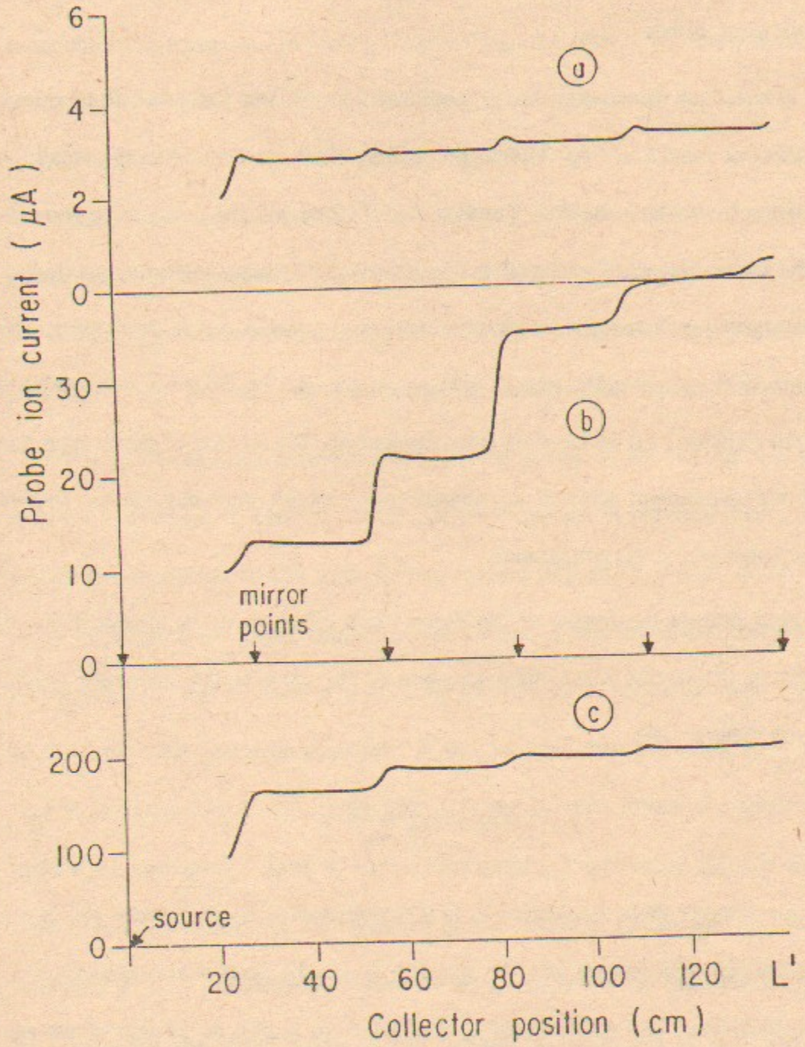

Figure 7. Langmuir probe ion saturation current (proportional to n) in the first cell as a function of the collector position in (a) low density, (b) intermediate density, and (c) high density regimes, for a 5 cell multiple mirror device.

collisional MHD flow, respectively. These regimes were confirmed by measurements with sliding axial probes.

The Novosibirsk installation had a length of 240 cm and consisted of 14 mirror cells with mirror ratio $k = 1.83$. The range of densities corresponded to the condition $\lambda \geq l$, which allowed both the free Knudsen flow regime and the small scale corrugation regime to be studied. Sometimes the boundary of the large scale regime (hydrodynamical regime) was reached.The experiments were carried out in both the steady state regime [62], and impulse regime [63], when the plasma behavior was analyzed after a rapid switching off of the flow from the ionizer. The method of performing and analyzing the experiment allowed a comparison of theory with experiment without exact knowledge of the ion temperature.

We now discuss the results of the Novosibirsk experiments in greater detail. If everywhere in the device $\lambda > l$, then equation (2.28) predicts the stationary density profile to be exponential:

$$n(z) = n_L \exp\left[\frac{L - z}{\lambda_L}\right], \tag{5.1}$$

where z is a distance from the ionizer, L is the coordinate of the last probe which was located in the cell with number $N = 11$, n_L, and λ_L are the plasma density and the ion mean free path (the exact definition of λ_L follows from (2.28)) at the exit of the system $z = L$. It follows from (5.1) that for $\lambda_L \ll L$ the plasma density near the ionizer is much greater than the density n_L. This theoretical variation was checked experimentally.

The results of the measurements of the plasma density distributions confirmed the exponential dependence of $n(z)$. Calculating the slope of the linear function $\ln(n(z)/n_L)$ the value of λ_L was found for a given experiment. In this way λ_L is calculated without using the ion temperature. This λ_L was then checked for self-consistency with the assumption leading to (5.1). With this treatment of the measurements for each experiment, the dependence $n(0)/n_L = f(L/\lambda_L)$ was then found from the results of a number of experiments. The value of λ_L and the correspondingly n_L was varied from one experiment to another by changing the plasma flux at the ionizer.

The results of measurements are illustrated in Fig. 8. As one can see, over a reasonably wide range of parameters there is good agreement between theory and experiment. The transition to the high density regime ($\lambda_L \ll l$) proved to be difficult to reach because of the appearance of plasma losses. Some deviation from the exponential dependence that occured at a small λ_L seemed to be concerned with the beginning of the large-scale corrugation regime. If this happens then the small scale approximation is violated first within some area near the ionizer, where the approximation of large-scale corrugation starts to apply. Some theory, developed for this situation and based on the matching of the solution of the equation (2.28) and (3.23) across the boundary $\lambda \simeq l$, predicts the existence of a maximum for the function $f(L/\lambda_L)$ at $\lambda_L \sim Nl$. The maximum value of this function is estimated as $N/(2\ln N)^{1/2}$, which gives $(n(0)/n_L)_{\max} \simeq 5$ at $N = 11$, in a reasonable agreement with the results presented by Fig. 8. In summary, the experiments with an alkali plasma not only qualitatively but also quantitatively confirmed the validity of the multiple mirror confinement theory.

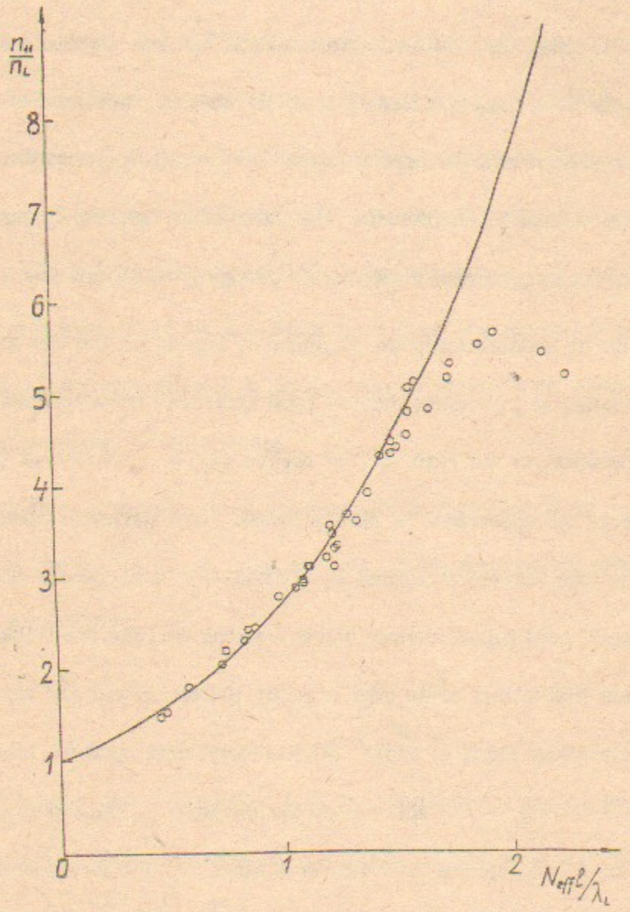

Figure 8. Comparison of theory and experiment for $n(0)/n_L$ as a function of L/λ_L.

The Berkeley multiple mirror alkali device was later modified for experiments with hydrogen plasma. A conical θ-pinch was used as a plasma source that allowed a density within the range $n \simeq 10^{12} - 10^{14}$ cm^{-3} at a temperature $T = 10$ eV to be obtained. The geometrical characteristics of the device and the number of cells in it were practically the same as in the experiments with alkali plasma. The magnetic field configuration was reconstructed into a set of the nonaxisymmetric mirror cells with an average min-B. This was done for stabilization of the MHD flute perturbation which was absent in the alkali plasma because of the contact with the ionizer. The main purposes of this set of experiments [64] was an analysis of the MHD stability and the measurement of transient confinement at higher density and temperature in the presence of radial and axial plasma losses. A quantitative comparison of the axial loss with the theoretical prediction was difficult because of the small number of mirror cells and the small length of each of them.

This difficulty was decreased in a larger installation which had a full length (including sources) $L = 10$m, $N = 9$, $l = 75$ cm [65]. The magnetic system provided the nonaxisymmetric magnetic field with a small mirror scale length $l_m = 10$ cm, that made it possible to realize all of the plasma confinement regimes, including the "ideal" one (Section 3.2). Plasma sources at each end consisted of a θ-pinch and a plasma gun, respectively, providing initial density values up to $n \simeq 10^{15}$ cm^{-3} at a temperature $T \simeq 3 - 8$ eV. The probe measurements, which were made simultaneously in many cells, allowed the time and the spatial plasma bunch evolution to be measured during the expansion along field lines. Since the density decreased with time, the various regimes of the plasma motion could be observed from the large scale to the

small scale. The comparison of the numerical calculations using (2.28) and (3.23) with the experimental dependences $n(z,t)$ gave good quantitative agreement [66]. This conclusion relates to the moderate density range $n \lesssim 10^{13}\,\mathrm{cm}^{-3}$. At high densities $n \simeq 10^{14} - 10^{15}\,\mathrm{cm}^{-3}$, when plasma flow was pure hydrodynamic, the comparison of axial confinement theory with the experiment could not be done because the plasma was dominated by radial losses.

A set of experiments on multiple mirror confinement were also carried out at Nagoya University [67–69]. Using a small installation with L = 1m, N = 10, l = 10 cm they could observe at $n = 10^{14}\,\mathrm{cm}^{-3}$ and $T \simeq 10$ eV the regime of large scale corrugation ($\lambda < l$).

The experimental results summarized above generally confirm the theory in practically all of the regimes of multiple mirror confinement. These conclusions hold both for experiments with alkali plasma and for experiments with hydrogen plasma.

The experiments, in which the plasma was not stabilized by line tying, were also useful in checking the predictions of MHD stability. A set of quadrupole coils of the type investigated theoretically [56] (see Fig. 6) were installed on the first Berkeley experiment. Because of design constraints of the existing magnets it was not possible to obtain complete stabilization with the added quadrupoles. The resulting confinement system was tested both using an alkali plasma that was disconnected from the ionizing source, and with a hydrogen plasma created by a θ-pinch source. For both types of plasmas a flute instability was clearly seen when the quadrupole coils were not activated. The flutes were not totally stabilized, as expected, when the quadrupole coils

were activated, but the reduction in growth rate predicted by the theory was observed [70].

MHD stability studies were also undertaken in the Berkeley 10 m device. The coil design for this system included fully stabilizing weak and strong quadrupoles such that an ave-min-B magnetic field was achieved over a range of mirror ratios. The experiments indicated that stable plasmas could be achieved up to the highest β's obtained by the counterstreaming θ-pinch and Marshal gun hydrogen sources ($\beta > 25\%$) [57]. Other ave-min-B magnetic field configurations, with longer connection lengths, were also tested, and found to go unstable at lower values of β, as predicted theoretically [57, 58]. The conclusion of these studies was that ave-min-B coils structures could be designed to stabilize magnetically confined plasmas up to $\beta \sim 1$.

SUMMARY AND DISCUSSION

A theory of plasma diffusion through a corrugated magnetic field (multiple mirrors) has been developed, that is applicable to the complete range of ratio of mean free path to cell length, and of mirror ratios. Estimates of the local flow rate, and therefore the local diffusion, are given in Section 1. These regimes naturally divide, for study, into the long mean free path regime ("small scale corrugation") with $\lambda/l \gg 1$, and the short mean free path regime ("large scale corrugation") with $\lambda/l \ll l$, and are treated rigorously in Sections 2 and 3, respectively. Analytic results can be obtained for the cases of $k \gg 1$ (strong corrugation) and $k \ll 1$ (weak corrugation). The results are summarized in Table 4.

A case of considerable importance for the application of plasma confinement in multiple mirrors to fusion reactors occurs if the scale length of the individual mirrors l_m is much less than the length of an individual mirror cell l. In this case the inequality $l_m \ll \lambda \ll l$ can be satisfied, such that the individual cells are collisional but the mirror regions are collisionless. The resulting confinement properties are very favorable for reactor design, particularly for the steady-state concept, and has been called the "ideal" multiple mirror regime. The analysis of this case is presented in Section 3.3. The flow velocity found there is approximately

$$u \approx \frac{l/k}{L} v_{Ti}$$

which, for $l/k \ll L$, is a dramatic improvement over the free flow. The results for this case are also given in Table 4.

TABLE 4 Summary Table of Local Diffusion Coefficients D

$$\left(u = -D \frac{1}{n} \frac{dn}{dz} \right), \qquad \tau_{mm} \equiv L^2/D$$

	$\lambda \ll l_m, l$	$l_m \ll \lambda \ll l$ (point mirrors)	$\lambda \gg l$
$\lambda \gg lk$	$\frac{5}{6} \nu_{Ti} \frac{l l_m}{\lambda k \ln k}$		
$k \gg 1$	$.9 \nu_{Ti} \lambda/k^2$	$\frac{8}{9}\left(\frac{2}{\pi}\right)^{1/2} \frac{l}{k} \nu_{Ti}$	$\left(\frac{2}{\pi}\right)^{1/2} \frac{l}{k} \nu_{Ti}$
$\lambda \gg l/(k-1)^{3/2}$			$l \ll \lambda \ll l/(k-1)^{3/2}$
$k - 1 \ll 1$ sinusoidal mirrors	$1.1 \nu_{Ti} \lambda/(k-1)^{1/2}$	$\frac{3.3}{\pi^2} \nu_{Ti} l^2/\lambda (k-1)^2$	$\left(\frac{2}{\pi}\right)^{3/2} \nu_{Ti} l/(k-1)^2$
$k \gg 1$		$l/k \ll \lambda \ll lk$	$\lambda \ll l/k$

$\lambda \equiv T^2/(e^4 \Lambda n)$ $\qquad l_m \equiv (1/B)dB/dz$ $\qquad \nu_{Ti} \equiv (T/m_i)^{1/2}$,

Detailed studies of axial confinement in both pulsed and steady-state reactors have been made, using the results presented in Sections 2 and 3, or similar results obtained from alternate calculations. The basic procedure is to find a feasible configuration and then to optimize the variable parameters to obtain a device with minimum length at a given value of Q. The pulsed concept uses very high densities ($\beta \gg 1$) in which the magnetic field, in addition to supplying the magnetic mirrors, also thermally insulates the plasma from the wall which contains the plasma pressure. The procedure for calculating the axial confinement is outlined in Section 4.1 and the results of the optimizations are given in Table (2). The steady-state concept relies on magnetic confinement with the wall far from the plasma. The plasma density is limited by the necessity of balancing the plasma pressure with the magnetic pressure. The calculation procedure is outlined in Section 4.3 and the optimized parameters given in Table (3).

Each of the main reactor concepts have some special features that must be considered separately. Since the pulsed reactor operates with $\beta \gg 1$ on axis, the questions of plasma displacement of the magnetic field and of radial heat conduction to the wall become critical. Both of these questions have been considered in detail, and the results appear to be favorable for reactor operation. An important advantage of the pulsed concept is that the wall provides stability againts MHD modes in an axisymmetric magnetic field. This stabilization is sensitive to the overall configuration, and therefore has been carefully analyzed. These analyses are discussed and results given in Section 4.2. A main consideration in a magnetically confined steady-state reactor is MHD stability. Stabilization requires the use of linked quadrupoles which give distorted

magnetic surfaces and a limited range of stabilization. In addition, the resulting field is only ave-min-B and therefore may be subject to ballooning modes for $\beta \simeq 1$. Calculations indicate the well radius is sufficiently large for reactor operation. Because of the short connection length between good and bad curvature regions, ballooning modes are found to be stable up to $\beta \lesssim 1$. Finally, radial diffusion, which is enhanced because of the fanned magnetic field, is found to be acceptable at a reactor design value of $\beta = 0.8$. The results are summarized in Section 4.4.

The basic confinement theory has been checked, experimentally in most of the confinement regimes discussed. Because $\lambda \propto T^2/n$ it is quite easy to scale the mean free path to laboratory plasmas that operate over the range of values of λ/l. This was initially done in steady state Alkali plasmas with simple mirrors, in which the plasma was stabilized by line-tieing to the ionizing source. Reasonable agreement between theory and experiment was obtained, over the complete range $1 \ll \lambda/l \ll 1$, with mirrors that had a single scale length. Later, the important regime $l_m < \lambda < l$ was investigated with a 10 meter device in which $l_m \ll l$, giving good agreement with theory. In this device a pulsed hydrogen source was used to create the plasma, which therefore had to be stabilized with quadrupoles. The stabilization was achieved in agreement with the theoretical predictions of ave-min-B stability. The plasma was also stabilized up to the highest β obtainable in the device ($\beta \sim 0.25$) in agreement with the predictions of ballooning theory. These results are discussed and summarized in Section 5.

The results given in Tables (2) and (3) for the parameters of pulsed and steady-state reactors are feasible and competitive with the Tokamak concept. Nevertheless, there are various features that are not desirable. Consequently many suggestion have

been made to improve the reactor operation or otherwise to modify the less desirable aspects of the reactors. Although optimization procedures were employed for minimizing the reactor length, certain parameters were held fixed, without optimization. For example, β was considered fixed at the value $\beta = 0.8$ for the steady-state reactor calculation. If we assume classical losses between unlike charged particles only, then the confinement time scaling with β for axial loss τ_z and radial loss τ_r is as follows: $\tau_z \propto (1-\beta)^{-1}$ and $\tau_r \propto 1-\beta$. Approximating the total confinement time as $1/\tau \approx 1/\tau_z + 1/\tau_r$, then τ is maximized for $\tau_r = \tau_z$. We can therefore vary β to achieve this condition. For an axisymmetric device this optimization has been performed [54] indicating some improved confinement could be achieved, particularly for the wetwood burner concept.

More radical methods of achieving improved performance have also been proposed. One method mentioned briefly at the end of Section 2.3 involved the creation of traveling-wave mirrors [20]. It was shown that mirrors traveling at the expansion speed of the plasmoid could essentially stop the expansion. A steady-state version of this idea were also examined [30] under different assumptions, and it was found that large improvements in confinement could be achieved. An important limitation on this type of confinement, which was not discussed by either of the above authors, is plasma heating. The time varying mirror fields magnetically pump the plasma, which, together with collisions, lead to irreversible energy transfer [71]. A simplified analysis of the containment time τ_{tw} with traveling-wave multiple mirrors gives [71]

$$\tau_{tw} = \frac{1}{v_0}\left[\frac{p}{v_0}\left(e^{\frac{v_0}{D}\frac{L}{2}} - 1\right) - \frac{L}{2}\right] \tag{1}$$

where v_0 is the mirror velocity and D (assumed independent of n) is the diffusion coefficient in the absence of v_0. For v_0 significantly greater than $v_L = 2D/L$, the flow velocity in the absence of moving mirrors, the exponential term dominates the behavior, giving

$$\tau_{tw}/\tau_{mm} \approx (v_L/v_0)^2 \exp(v_0/v_L) \gg 1. \tag{2}$$

To obtain the heating we use the magnetic pumping equations [72] giving

$$\tau_h \approx \frac{1}{2\pi^2(R-1)^2}\left[\frac{l_c}{v_0\tau_{ii}}\right]^2 \tau_{ii}. \tag{3}$$

We use the restriction that $\tau_h \leq \tau_{tw}/8$ to prevent overheating and find that the improvement in confinement is limited to about $\tau_{tw}/\tau_{mm} \approx 3$. This improvement, although not dramatic, is still interesting, and merits a more exact calculation.

The traveling mirror concept is a specific example of the general concept of producing asymmetric scattering. If the random walk distance that an ion moves could be made asymmetrical such that it moves further towards the center of the device than towards the ends, a large improvement in confinement can theoretically be obtained. The scaling for an arbitrary asymmetry was examined for the special case of a large central cell, with the end cells used for confinement, only, to obtain the ratio of the confinement to the center cell confinement [73]

$$\tau_{\text{eff}}/\tau_0 = [1 + (1 - p_0)N^*] \tag{4}$$

where $N^* = (k_1^N - 1)(k_1 + k_2 - 1)(k_1 - 1)$, $k_1 = f_c/f_e$, $k_2 = 1 - f_c/f_e$, where f_c and f_e are the probabilities of escape toward the center and end, and p_0 the probability of a particle being untrapped in the center cell. For k_1 large, N^* and therefore τ_{eff}/τ_0 are very large. The authors did not clearly demonstrate that such an asymmetry could be produced, but they reasoned physically that one non-adiabatic and one adiabatic mirror should produce an asymmetry. Although the asymmetry achieved in this manner is likely to be small, it can still have a significant effect on confinement. For example, a 10 percent asymmetry with ten mirror cells will give a $\tau_{eff}/\tau_0 \approx 2$. Clearly more detailed calculations of the amount of asymmetry that can be achieved in this manner should be undertaken.

Another interesting possibility is collision independent scattering. We have seen that the power loss for collisional scattering has the temperature proportionality $P_l \propto T^{7/2}$. For collision independent scattering, if we assume that the random walk distance l_z is independent of n and T, then the multiple-mirror confinement time has the proportionality $\tau_{mm} \approx L^2/v_T l_z \propto T^{-1/2}$ and the power loss $P_l \propto nT^{3/2} l_z$. An optimum temperature of $T_{opt} \approx 15$ keV, was found [74]. The more favorable temperature allows significant reduction in density and therefore in B. If l_z can be made significantly smaller than that for the comparable collisional reactor further improvements are possible.

One method of achieving collision independent scattering is to have sharp gradients in the d.c. magnetic field. These are further enhanced by high β. However, the nonadiabaticity is strongly energy dependent, only scattering the higher energy particles. Although some improvement can be achieved in this manner, dramatic

improvement requires non-adiabaticity of the lower energy particles, also. A method of obtaining non-adiabatic scattering, particularly suitable to lower energy particles, is by cyclotron resonance heating (CRH). If we assume that the fields can penetrate into the plasma at the ion cyclotron resonance, which appears to be possible, then the collision independent scattering process works as follows: Rapid stochastic heating is obtained up to a stochastic energy W_s Beyond this energy, slower heating takes place up to a barrier energy $W_b = 5W_s$, with the steady-state energy distribution function having a maximum around W_s. Individual particles rapidly diffuse both up and down in their perpendicular velocity, thereby scattering in and out of the loss cone, thus giving a short effective random walk distance for energies below W_b. However, on a collisional time scale the plasma is heated beyond W_b, which can lead to overheating. An analysis of a reactor employing this mechanism indicated a modest improvement in confinement time of about a factor of 2 [75].

In conclusion, multiple mirror devices hold considerable promise for confining fusion plasmas. They have the specific advantages of simplicity, and ease in extending the confinement time by increasing the device length. The fundamental confinement theory has been worked out in detail. Using the results of the confinement calculations, both pulsed and steady-state reactor concepts have been developed and appear to be feasible.

References

1. Budker, G. I., "Thermonuclear Reactions in a System with Magnetic Stoppers and the Problem of Direct Transformation of Thermonuclear Energy into Electrical Energy," *Plasma Physics and the Problem of Controlled Thermonuclear Reactions*, Pergamon Press, New York, 1959, vol. III, pp. 1–33.
2. Post, R. F., Proc. of Second U.N. Int. Conf. on Peaceful Uses of Atomic Energy, Geneva, 1958, vol. 32, p. 245.
3. Dimov, G. I., Zakaidakov, V. V., and Kishinevskii, M. E., *Fizika Plasma* **2,** (1976), p. 597.
4. Fowler, T. K. and Logan, B. G., *Comments on Plasma Physics and Controlled Fusion*, **2,** (1977), p. 167.
5. Kadomtsev, B. B., "Magnetic Traps with a 'Corrugated' Field," *Plasma Physics and the Problem of Controlled Thermonuclear Reactions*, Pergamon Press, New York, 1959, vol. III, pp. 340–355.
6. Tuck, J. L., "Monte Carlo and Computer Plasma Simulation Studies of the Inhibition of End Loss from a θ-pinch by Non-adiabatic 'Rough' Magnetic Walls," Rep. CN-24/K-5 on 3rd Intl. Conf. on Plasma Physics and Controlled Thermonuclear Fusion, Novosibirsk (1968), vol. 2, pp. 595–605.
7. Post, R. F., "Confinement of Charged Particles by Multiple-Mirror Systems," *Phys. Rev. Lett.* **18,** (1967), pp. 232–236.
8. Logan, B. G., Lichtenberg, A. J., and Lieberman, M. A., "Multiple-Mirror Confinement for Fusion Reactors," *Bull. Amer. Phys. Soc.* **15,** (1970), p. 1432.
9. Logan, B. G., Lichtenberg, A. J., and Lieberman, M. A., "Multiple-Mirror Confinement of Plasmas," *Phys. Rev. Lett.* **28,** (1972), pp. 144–147.
10. Makhijani, A., Lichtenberg, A. J., Lieberman, M. A., and Logan, B. G., "Plasma Confinement in Multiple-Mirror Systems. I: Theory," *Phys. Fluids* **17,** (1974) pp. 1291–1301.
11. Budker, G. I., Mirnov, V. V., and Ryutov, D. D., "The Influence of Magnetic Field Corrugation on the Expansion and Cooling of a Dense Plasma," *JETP Lett.* **14,** (1971), pp. 320–324 (in Russian).
12. Mirnov, V. V. and Ryutov, D. D., "Gas-dynamic Description of a Plasma in a Corrugated Magnetic Field," *Nucl. Fus.* **12,** (1972), p. 627.
13. Breizman, B. N., Mirnov, V. V., and Ryutov, D. D., "Ohmic Resistance of an Inhomogeneous Plasma," *Soviet Physics JETP*, vol. 31, No. 5, (1970), p. 948.
14. Mirnov, V. V., "Electroconductivity and Skin-effect in Corrugated Magnetic Field," *Collection of abstracts of the Int. Conf. on Closed Systems Plasma Confinement*, Dubna, (1969) 53 (in Russian).
15. Mirnov, V. V., "Skin Effect in a Corrugated Magnetic Field," *Nucl. Fus.* **11,** (1971), pp. 221–230.

16. Budker, G. I., Kruglyakov, E. P., Mirnov, V. V., and Ryutov, D. D., "On the Possibility of a Thermonuclear Reactor with a Dense Plasma Contained by Corrugated Magnetic Field," In Proc. of USA-USSR Seminar on System Analysis and Thermonuclear Power Station Construction, Leningrad, 1974 (in Russian), *Izvestija Ak. Nauk SSR - Energetics and Transport*, 6 (1975), pp. 35–40 (in Russian).
17. Galeev, A. A. and Sagdeev, R. Z., "Transport Phenomena in a Collisionless Plasma in a Toroidal Magnetic System," *Soviet Physics JETP*, vol. 26, No. 1, (1968), p. 233.
18. Braginskii, S. I., "Transport Processes in a Plasma," in *Reviews of Plasma Physics*, (Voprosy teorii plazmy) Consultants Bureau, N.Y., 1965, vol. 1, pp. 205–311.
19. Dawson, J. M., Hertzberg, A., Kidder, R. E., Vlasses, G. G., Ahlstrom, H. G., and Steinhauer, L. G., "Long-wavelength, High-powered Lasers for Controlled Thermonuclear Fusion," Report CN-28/D-13 on 4th Intern. Conf. on Plasma Physics and Controlled Thermonuclear Fusion, Madison (1971), vol. 1, pp. 673–687.
20. Budker, G. I., Mirnov, V. V., and Ryutov, D. D., "Gas-dynamics of a Dense Plasma in Corrugated Magnetic Field," *Proc. of the Int. Conf. on Plasma Theory*, Kiev (1972), pp. 145–151 (in Russian).
21. Mirnov, V. V. and Ryutov, D. D., "Expansion of a Plasma along a Weakly Corrugated Magnetic Field," *Proc. 5th Europ. Conf. on Plasma Physics and Controlled Thermonuclear Fusion*, Grenoble, I, (1972) p. 100.
22. Budker, G. I. and Beliaev, S. T., "Boltzmann's Equation for Electron Gas in which Collisions are Infrequent," *Plasma Physics and the Problem of Controlled Thermonuclear Reactions*, Pergamon Press, New York, 1959, vol. II, pp. 431–457.
23. Zakharov, V. E. and Karpman, V. I., "On the Nonlinear Theory of the Damping of Plasma Waves," *Soviet Physics JETP*, vol. 16, No. 2, (1963), p. 351.
24. Hinton, F. L. and Oberman, C., "Electrical Conductivity of a Plasma in a Spatially Inhomogeneous Magnetic Field," *Nuclear Fusion*, 1969, vol. 9, No. 4, pp. 319–327.
25. Vekstein, G. E., Ryutov, D. D., Spektor, M. D., and Cheboteev, P. Z., "Nonmagnetic Containment of a Dense Plasma," *J. of Applied Mechanics and Technical Physics*, vol. 15, No. 6, (1974), pp. 731–739.
26. Vekstein, G. E., Mirnov, V. V., Ryutov, D. D., and Chebotaev, P. Z., "Theory and Calculations of Non-magnetic Dense Plasma Confinement," Proc. of 6th Int. Conf. on Plasma Phys. and Contr. Nucl. Fus. Research, Munich, 1976. Vienna IAEA, 1977, CN-351E-21, vol. 3, pp. 535–545.
27. Vekstein, G. E., "Magnetothermal Processes in Dense Plasma," in *Reviews of Plasma Physics* (Voprosy teorii plazmy), Consultants Bureau, N.Y., 1990, vol. 15, pp. 1–57.
28. Seyler, C. E., Grossman, W., and Steinhauer, L. C., "End Stoppering by the Reversed Field Multiple-Mirror Concept," *Comments Plasma Phys. Conf. Fus.*, 4

(1978) p. 21.

29. Musher, S. L. and Spector, M. D., "Transverse Confinement of a High Pressure Plasma in a Corrugated Magnetic Field," *Nuclear Fusion*, 1980, vol. 20, No. 2, pp. 149–157.
30. Aihara, S., "Travelling Wave Multiple Mirror Field for Confinement of High Temperature Plasmas," Research Report, Institute of Plasma Physics, Nagoya University, IPPJ-234, November, 1975.
31. Galeev, A. A. and Sagdeev, R. Z., "Nonlinear Plasma Theory," in *Reviews of Plasma Physics* (Voprosy teorii plazmy), Consultants Bureau, N.Y., 1979, vol. 7, p. 88.
32. Shapiro, D. A., "Equations of Motion of a Plasma in a Slightly Bumpy Magnetic Field," *Sov. J. Plasma Phys.*, 1977, **3**, No.3, pp. 545–550.
33. Bravenec, R. V., Lichtenberg, A. J., Lieberman, M. A., and Berk, H. L., "Viscous Plasma Flow in a Multiple-Mirror Configuration," *Phys. of Fluids* **24**, (7), 1981, pp. 1320–1325.
34. Bravenec, R. V., Berk, H. L. and Hammer, J. H., "An Alternative Derivation of the Parallel Ion Viscosity," *Phys. of Fluids* **25**, (4) 1982, p. 608–609.
35. Vasiljev, Yu. V. and Mirnov, V.V., "Gas-Dynamics of a Plasma in Multiple-Mirror Magnetic Trap with 'Point Mirrors'," *J. of Applied Mechanics and Technical Physics*, N 6 (1974), pp. 14–19.
36. Najmabadi, F., Lichtenberg, A. J., and Lieberman, M. A., "Effect of Ambipolar Potential on Multiple Mirror Confinement," *Physics of Fluids* **26**, 4, 1983, pp. 1018–1027.
37. Budker, G. I., Danilov, V. V., Kornilov, V. A., Kruglyakov, E. P., Lukyanov, V. N., Mirnov, V. V., and Ryutov, D. D., "Confinement in a Multiple-Mirror Magnetic Field," Report CN-33/H8-3 on 5th Intern. Conf. on Plasma Physics and Controlled Thermonuclear Fusion, Tokyo, vol II, (1974), pp. 763–776.
38. Dawson, J. M., Kidder, R. E., and Hertzberg, A., Preprint MATT-782, Plasma Physics Lab., Princeton University, 1971.
39. Logan, B. G., Brown, I. G., Lichtenberg, A. J., and Lieberman, M. A., "Plasma Confinement in Multiple-Mirror Systems. II: Experiment and Reactor Calculation," *Phys. Fluids* **17**, (1974), pp. 1302–1313.
40. Mirnov, V. V. and Ryutov, D. D., "The Effect of Heavy Impurities on Plasma Motion in a Multiple Mirror Magnetic Field," Proc. 7th Europ. Conf. on Plasma Physics and Controlled Thermonuclear Fusion, Lausanne (1975), p. 143.
41. Chebotaev, P. Z., Knyazev, B. Z., Mirnov, V. V., and Vekstein, G. E., "Plasma Confinement Optimization in a Multiple-Mirror Magnetic Trap," Proc. of the X European Conf. on Controlled Fusion and Plasma Physics, Moscow, 1981, vol. 1, C-6.
42. Knyazev, B. A., Mirnov, V. V., and Chebotaev, P. Z., "The Improvement of Longitudinal Plasma Confinement in Multiple-Mirror Trap," Preprint INP

Novosibirsk, No. 81-100, 1981 (in Russian), *Voprosy atomnoi nauki i tekhniki. Termoyadernij sintez* **3**, (13), 1983, pp. 12–17.

43. Budker, G. I., "Thermonuclear Fusion in Installations with a Dense Plasma," *Proc. 6th Europ. Conf. on Plasma Physics and Controlled Thermonuclear Fusion*, Moscow, 2 (1973), pp. 146–158,
44. Knyazev, B. A. and Chebotaev, P. Z., "Pulsed Multi-Mirror Fusion Reactor: Longitudinal Confinement," *Nuclear Fusion*, 1984, vol. 24, No. 5, pp. 555–563.
45. Yang, S. T. and Lieberman, M. A., "Power Balance and Impurities in Two-component, Multiple-mirror Reactors," *Nucl. Fus.*, 17 (1977) pp. 697–712.
46. Vasil'ev, Yu. V. and Ryutov, D. D., "High-energy Part of Ion Distribution Function in a Multiple-Mirror Magnetic Trap," *J. of Applied Mechanics and Technical Physics*, **18**, No. 3, (1977), pp. 295–299.
47. Vekshtein, G. E., Ryutov, D. D., and Chebotaev, P. Z., "Diffusion of Heavy Impurities in a Dense, Wall-Confined Plasma," **1**(3), (1975), pp. 220–222.
48. Spector, M. D., "Hydrodynamic Stability of Dense Plasma in a Corrugated Magnetic Field," *J. of Applied Mechanics and Technical Physics*, **16**(1), 1975, pp. 22–30.
49. Ryutov, D. D., "The Study of Open-Ended Fusion Systems in Novosibirsk Institute of Nuclear Physics," *Voprosy atomnoi nauki i tekhniki. Termoyadernij sintez*, N 1–2 (1978) pp. 96–112, (in Russian).
50. Krivosheev, M. V., Komin, A. V., Krylov, C. N., Seko, E. V., Knyazev, B. A., and Ryutov, D. D., "Parameter Studies of the Power Installation Based on Multiple Mirror Trap," *Voprosy atomnoi nauki i tekhniki. Termoyadernij Sintez*, 1982, 2(10), pp. 2–16.
51. Yang, S. T. and Lieberman, M. A., "Two-component, Multiple-mirror Reactor with Depressed Ion Temperature," *Nucl. Fus.*, 18 (1978) pp. 965–969.
52. Najmabadi, F., Lichtenberg, A. J., and Lieberman, M. A., in *Engineering Problems of Fusion Research*, Proc. 8th Symp. San Francisco, California, November 1979, IEEE, vol. 2 (1979) 632.
53. Najmabadi, F., Lichtenberg, A. J., and Lieberman, M. A., "Parameter Optimization of Multiple-mirror Reactors," *Nuclear Fusion*, 1983, vol. 23, No. 5, pp. 609–631.
54. Tuszewski, M. and Lieberman, M. A., "Radial Losses in High-β Multiple Mirror Plasmas," *Phys. Fluids*, **24**, (2), 1981, pp. 320–327.
55. Zawaideh, E. S. "Generalized Fluid Equations for Parallel Transport in Collisional to Weakly Collisional Plasmas," Ph.D Thesis, University of California, Los Angeles, (1985).
56. Riordan, J. C., Lichtenberg, A. J., and Lieberman, M. A., "Minimum-average-B Wells in Linked Magnetic Mirror Fields," *Nucl. Fus.*, 19 (1979), pp. 21–31.
57. Price, H. D., Benjamin, M. P., Kang, B. K., Lichtenberg, A. J., and Lieberman, M. A., "A Study of High Beta Ballooning Modes," *Physics of Fluids*, **28**(1),

1985, pp. 392–408.

58. Kang, B. K., Lichtenberg, A. J., and Nevins, W. M., "Resistive Effects on Rigid Mode Ballooning Instability," *Phys. Fluids*, **30,** (1987), pp. 1415–1429.

59. Tuszewski, M. and Lichtenberg, A. J., "Two-dimensional Boundary-value Problem for Ion-ion Diffusion," *Phys. Fluids*, **20,** (1977), pp. 1263–1274.

60. Logan, B. G., Brown, I. G., Lieberman, M. A., and Lichtenberg, A. J., "Experimental Evidence of Multiple-mirror Plasma Confinement," *Phys. Rev. Lett.*, **29,** (1972) 1435.

61. Budker, G. I., Danilov, V. V., Kruglyakov, E. P., Ryutov, D. D., and Shun'ko, E. V., "Experiments on Alkali Plasma Confinement in a Corrugated Magnetic Field," *JETP Lett.*, **17,** (1973) pp. 117–120 (in Russian).

62. Budker, G. I., Danilov, V. V., Kruglyakov, E. P., Ryutov, D. D., and Shun'ko, E. V., "Experiments on Plasma Confinement in a Magnetic Multi-Mirror Trap," *Sov. Phys. JETP*, **38**(2), (1974), pp. 276–282.

63. Danilov, V. V. and Kruglyakov, E. D., "Plasma Dynamics in a Multi-Mirror Magnetic System," *Sov. Phys. JETP*, **41**(6), (1975), pp. 1055–1058.

64. Tuszewski, M., Lichtenberg, A. J., and Eylon, S., "Transient Confinement of a High Density Plasma in a Multiple Mirror Magnetic Field Configuration," *Nuclear Fusion*, 1977, vol. 17, No. 5, pp. 893–902.

65. Tuszewski, M., Price, D., and Lieberman, M. A., "MHD-stabilization of Finite β Multiple-mirror Plasmas," *Nuclear Fusion*, 1979, vol. 19, No. 9, pp. 1244–1247.

66. Price, H. D., Lichtenberg, A. J., Lieberman, M. A., and Tuszewski, M., "Radial and Axial Losses in a Multiple-Mirror Experiment," *Nuclear Fusion*, 1983, vol. 23, No. 8, pp. 1031–1052.

67. Inutake, M., Komori, A., Hatakeyama, R., and Sato, N., "Stability of High Density Plasma in a Multiple Mirror," 9th European Conf. on Contr. Fusion and Plasma Physics, Oxford, 1979, p. 51.

68. Komori, A., Inutake, M., Hatakeyama, R., and Sato, N., "High Density Plasma Confinement in a Multiple Mirror," *Physics Lett.*, 1980, vol. 78A, No. 2, pp. 143–144.

69. Hatakeyama, R., Inutake, M., and Sato, N., "Low-Frequency Plasma Instability in a Multiple-mirror Configuration," Proc. of Int. Symposium on Physics and Open-Ended Fusion Systems, Tsukuba, Japan, 1980, p. 313. *J. Phys. Soc. Japan*, 1980, vol. 48, No. 2, pp. 707–708.

70. Riordan, J. C., Tuszewski, M., and Lichtenberg, A. J., "Stabilization of Interchange Modes in Multiple-mirror Confined Plasmas," *Plasma Physics*, **20,** (1978), pp. 139–155.

71. Lichtenberg, A. J., "New Ideas in Multiple Mirror Confinement," Proc. Int. Symp. on Physics of Open-Ended Fusion Systems, Tsukuba, Japan (1980) p. 321.

72. Dawson, J. M. and Uman, M. F., *Nucl. Fusion*, **5,** (1965) p. 242.

73. Post, R. F. and Li, X. Z., "Particle Confinement in Asymmetric Cell Multiple-Mirror Systems," *Nucl. Fusion*, **21,** (1981) p. 135.

74. Lichtenberg, A. J. and Lieberman, M. A., "Multiple Mirror Confinement with Collision Independent Scattering," *Nucl. Fusion*, **16,** (1976) p. 532.

75. Donniger, K. J., Lieberman, M. A., and Lichtenberg, A. J., "A Theoretical Study of ICRF Effects on Multiple-Mirror Confinement," *Nucl. Fusion*, **25,** (1985) pp. 3–20.

Allan J. Lichtenberg, Vladimir V. Mirnov

Multiple Mirror Plasma Confinement

В.В. Мирнов, А.Лихтенберг

Многопробочное удержание плазмы

Ответственный за выпуск С.Г. Попов

Работа поступила 21 ноября 1990 г.
Подписано в печать 21.11 1991 г.
Формат бумаги 60×90 1/16 Объем 7,0 печ.л., 3,0 уч.-изд.л.
Тираж 270 экз. Бесплатно. Заказ N 116

Обработано на IBM PC и отпечатано на
ротапринте ИЯФ СО АН СССР,
Новосибирск, 630090, пр. академика Лаврентьева, 11.